

Achiral and Chiral Transition Metal Complexes with Modularly Designed Tridentate PNP Pincer-Type Ligands Based on N-Heterocyclic Diamines

David Benito-Garagorri,[†] Eva Becker,[†] Julia Wiedermann,[†] Wolfgang Lackner,[†] Martin Pollak,[†] Kurt Mereiter,[‡] Joanna Kisala,[§] and Karl Kirchner^{*,†}

Institute of Applied Synthetic Chemistry and Institute of Chemical Technologies and Analytics, Vienna University of Technology, Getreidemarkt 9, A-1060 Vienna, Austria, and Faculty of Chemistry, Rzeszów University of Technology, 6 Powstańców Warszawy Avenue, 35-959 Rzeszów, Poland

Received January 22, 2006

The synthesis and characterization of a series of molybdenum, iron, ruthenium, nickel, palladium, and platinum complexes containing new achiral and chiral PNP pincer-type ligands based on the N-heterocyclic diamines 2,6-diaminopyridine, *N,N'*-di-10-undecenyl-2,6-diaminopyridine, *N,N'*-dihexyl-2,6-diaminopyridine, and 2,6-diamino-4-phenyl-1,3,5-triazine are reported. The new PNP ligands are prepared conveniently in high yield by treatment of the respective N-heterocyclic diamines with 2 equiv of a variety of achiral and chiral R₂PCl compounds in the presence of base. Molybdenum PNP complexes of the type [Mo(PNP)(CO)₃PNP] are obtained by treatment of [Mo(CO)₃(CH₃CN)₃] with 1 equiv of the respective PNP ligand. They were found to react with I₂ to give novel seven-coordinate pincer complexes of the types [Mo(PNP)(CO)₃I]⁺ and [Mo(PNP)(CO)₂(CH₃CN)I]⁺ depending of whether the reaction is carried out in CH₂Cl₂ or CH₃CN. With [Fe(H₂O)₆](BF₄)₂ and 1 equiv of PNP ligand in acetonitrile dicationic complexes of the type [Fe(PNP)(CH₃CN)₃](BF₄)₂ are obtained. The *cis* and *trans* dichloride complexes [Ru(PNP)(PPh₃)Cl₂] are prepared by a ligand exchange reaction of [RuCl₂(PPh₃)₃] with a stoichiometric amount of the respective PNP ligand. Cationic PNP complexes of Ni(II), [Ni(PNP)Br]⁺Br⁻, were synthesized by the reaction of [NiBr₂(DME)] with 1 equiv of PNP ligand. In similar fashion, treatment of [M(COD)X₂] (M = Pd, Pt; X = Cl, Br) with 1 equiv of PNP ligand yields the cationic square-planar complexes [M(PNP)X]⁺X⁻. If the reaction is carried out in the presence of the halide scavenger KCF₃SO₃, complexes of the type [M(PNP)X]CF₃SO₃ are obtained, which are better soluble in nonpolar solvents than the analogous halide compounds. X-ray structures of representative Mo, Fe, Ru, Ni, and Pd PNP complexes have been determined. Finally, the use of the palladium complexes as catalysts for the Suzuki–Miyaura coupling of some aryl bromides and phenyl boronic acid has been examined.

Introduction

Tridentate PNP ligands in which the central pyridine-based ring donor contains –CH₂PR₂ substituents in the two ortho positions are widely utilized ligands in transition metal chemistry (e.g., Fe, Ru, Rh, Ir, Pd, Pt).^{1–10} In this family of ligands steric, electronic, and stereochemical parameters can be manipulated by modifications of the benzylic positions and/or the phosphino R groups so as to control the reactivity at the metal center. Stereochemical parameters, however, are comparatively difficult to modify and often require tedious multistep syntheses and expensive starting materials.^{3,5a} As part of our effort to create novel tridentate PNP pincer-type ligands in which the steric,

electronic, and stereochemical properties can be easily varied, we describe here the synthesis of a series of modularly designed PNP ligands based on N-heterocyclic diamines and R₂PCl that contain both bulky and electron-rich dialkyl phosphines as well as various P–O bond-containing achiral and chiral phosphine units.^{11,12} This methodology was originally developed for the

* To whom correspondence should be addressed. E-mail: kkirch@mail.zserv.tuwien.ac.at.

[†] Institute of Applied Synthetic Chemistry, Vienna University of Technology.

[‡] Institute of Chemical Technologies and Analytics, Vienna University of Technology.

[§] Rzeszów University of Technology.

(1) Dahlhoff, W. V.; Nelson, S. M. *J. Chem. Soc. A* **1971**, 2184.

(2) (a) Vasapollo, G.; Giannoccaro, P.; Nobile, C. F.; Sacco, A. *Inorg. Chim. Acta* **1981**, *48*, 125. (b) Steffey, B. D.; Miedaner, A.; Maciejewski-Farmer, M. L.; Bernatis, P. R.; Herring, A. M.; Allured, V. S.; Carperos, V.; DuBois, D. L. *Organometallics* **1994**, *13*, 4844. (c) Hahn, C.; Sieler, J.; Taube, R. *Chem. Ber.* **1997**, *130*, 939. (d) Hahn, C.; Vitagliano, A.; Giordano, F.; Taube, R. *Organometallics* **1998**, *17*, 2060. (e) Hahn, C.; Spiegler, M.; Herdtweck, E.; Taube, R. *Eur. J. Inorg. Chem.* **1999**, 435.

(3) Jiang, Q.; Van Plew, D.; Murtuza, S.; Zhang, X. *Tetrahedron Lett.* **1996**, *37*, 797.

(4) (a) Andreocci, M. V.; Mattogno, G.; Zanoni, R.; Giannoccaro, P.; Vasapollo, G. *Inorg. Chim. Acta* **1982**, *63*, 225. (b) Sacco, A.; Vasapollo, G.; Nobile, C.; Piergiovanni, A.; Pellinghelli, M. A.; Lanfranchi, M. *J. Organomet. Chem.* **1988**, *356*, 397. (c) Abbenhuis, R. A. T. M.; del Rio, I.; Bergshoef, M. M.; Boersma, J.; Veldman, N.; Spek, A. L.; van Koten, G. *Inorg. Chem.* **1998**, *37*, 1749.

(5) (a) Rahmouni, N.; Osborn, J. A.; De Cian, A.; Fisher, J.; Ezzamarty, A. *Organometallics* **1998**, *17*, 2470. (b) Sablong, R.; Newton, C.; Dierkes, P.; Osborn, J. A. *Tetrahedron Lett.* **1996**, *37*, 4933. (c) Sablong, R.; Osborn, J. A. *Tetrahedron Lett.* **1996**, *37*, 4937. (d) Barloy, L.; Ku, S. Y.; Osborn, J. A.; De Cian, A.; Fischer, J. *Polyhedron* **1997**, *16*, 291.

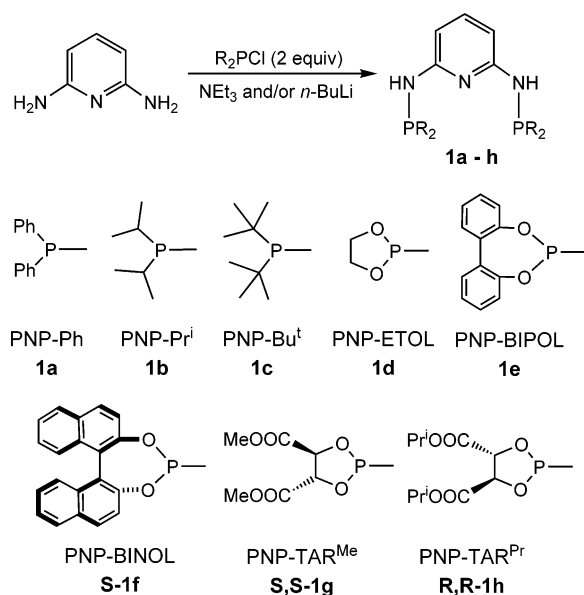
(6) (a) Zhang, J.; Leitius, G.; Ben-David, Y.; Milstein, D. *J. Am. Chem. Soc.* **2005**, *127*, 10840. (b) Zhang, J.; Gandelman, M.; Shimon, L. J. W.; Rozenberg, H.; Milstein, D. *Organometallics* **2004**, *23*, 4026. (c) Hermann, D.; Gandelman, M.; Rozenberg, H.; Shimon, L. J. W.; Milstein, D. *Organometallics* **2002**, *21*, 812.

(7) Gibson, D. H.; Pariya, C.; Mashuta, M. S. *Organometallics* **2004**, *23*, 2510.

(8) Katayama, H.; Wada, C.; Taniguchi, K.; Ozawa, F. *Organometallics* **2002**, *21*, 3285.

(9) Jia, G.; Lee, H. M.; Williams, I. D.; Lau, C. P.; Chen, Y. *Organometallics* **1997**, *16*, 3941.

Scheme 1



synthesis of *N,N'*-bis(diphenylphosphino)-2,6-diaminopyridine (PNP-Ph).¹³ Furthermore, we report the application of these ligands for the synthesis of a series of Mo, Fe, Ru, Ni, Pd, and Pt complexes. Some reactions of these new PNP compounds will be presented including preliminary results of the use of palladium PNP complexes in the catalytic cross-coupling of various aryl bromides with phenyl boronic acid (Suzuki–Miyaura coupling).

Results and Discussion

Ligand Synthesis. Similarly to the known ligand *N,N'*-bis(diphenylphosphino)-2,6-diaminopyridine (PNP-Ph), **1a**,¹³ the new PNP ligands **1b–h** are prepared conveniently in 64–95% yield by treatment of 2,6-diaminopyridine with 2 equiv of the respective $\text{R}_2\text{P-Cl}$ compound in the presence of base, viz., NEt_3 and/or *n*-BuLi (Scheme 1). Surprisingly, this methodology failed in the case of *N,N'*-dialkylated diaminopyridines. In fact, when the reaction of *N,N'*-dihexyl-2,6-diaminopyridine and *N,N'*-di-10-undecenyl-2,6-diaminopyridine and $\text{Ph}_2\text{P-Cl}$ was monitored by $^{31}\text{P}\{^1\text{H}\}$ NMR spectroscopy, no evidence for the formation of PNP-Ph^{Hex} (**2a**) and PNP-Ph^{Undec} (**2b**) was found; that is, P–N coupling did not occur, but instead several phosphorus-containing species were formed including tetraphenyldiphosphine (−16.1 ppm)¹⁴ and tetraphenyldiphosphine monoxide (doublet at 37 and −24 ppm with $J_{\text{PP}} = 229$ Hz) as a result of P–P coupling.¹⁵ The synthesis of these ligands could be achieved, however, via a two-step procedure. First, addition

of 1 equiv of $\text{Ph}_2\text{P-Cl}$ to *N,N'*-di-10-undecenyl-2,6-diaminopyridine and *N,N'*-dihexyl-2,6-diaminopyridine in the presence of *n*-BuLi afforded the monophosphinated compounds **2a'** and **2b'**, respectively. Subsequent addition of another equivalent of $\text{Ph}_2\text{P-Cl}$ and *n*-BuLi afforded then the desired PNP ligands **2a** and **2b** in high isolated yields (Scheme 2). Finally, the first PNP ligand with a 2,6-diamino-1,3,5-triazine backbone could be obtained by reacting 2 equiv of $\text{Ph}_2\text{P-Cl}$ with 2,6-diamino-4-phenyl-1,3,5-triazine, affording PNP^T-Ph (**3**) in 95% yield (Scheme 3).

All PNP ligands are air stable in the solid state and in oxygen-free solutions. They have been characterized by ^1H , $^{13}\text{C}\{^1\text{H}\}$, and $^{31}\text{P}\{^1\text{H}\}$ NMR spectroscopy. Most diagnostic is the $^{31}\text{P}\{^1\text{H}\}$ NMR spectrum, exhibiting one singlet in the range 28 to 143 ppm. In the ^1H NMR spectrum the NH protons of **1a–h** and **3** give rise to a slightly broadened doublet in the range 4.30 to 6.40 ppm. All other resonances are unremarkable and are not discussed here.

Molybdenum PNP Pincer Complexes. Molybdenum complexes featuring PNP pincer ligands are comparatively rare. A few years ago Haupt and co-workers reported the synthesis of $[\text{M}(\text{PNP-Ph})(\text{CO})_3]$ ($\text{M} = \text{Cr}, \text{Mo}, \text{W}$),¹³ while recently Walton and co-workers described the synthesis of the dinuclear molybdenum complex $[\text{Mo}(\text{PNP})\text{Mo}(\text{HPCy}_2)\text{Cl}_3]$ (PNP = 2,6-bis(dicyclohexylphosphinomethyl)pyridine).¹⁶ We prepared molybdenum tricarbonyl complexes with our new PNP ligands by reacting $[\text{Mo}(\text{CO})_3(\text{CH}_3\text{CN})_3]$, prepared in situ by refluxing a solution of $[\text{Mo}(\text{CO})_6]$ in CH_3CN for 4 h, with the PNP ligands **1a–c**, **2a**, and **3** to afford, upon workup, the complexes $[\text{Mo}(\text{PNP-Pr}^i)(\text{CO})_3]$ (**4a**), $[\text{Mo}(\text{PNP-Bu}^t)(\text{CO})_3]$ (**4b**), $[\text{Mo}(\text{PNP-TAR}^{\text{Pr}})(\text{CO})_3]$ (**4c**), $[\text{Mo}(\text{PNP-Ph}^{\text{Undec}})(\text{CO})_3]$ (**5**), and $[\text{Mo}(\text{PNP}^{\text{T}}\text{-Ph})(\text{CO})_3]$ (**6**) in 74 to 90% isolated yields (Scheme 4). With the exception of **4c**, all compounds are air-stable both in the solid state and in solution. **4c** slowly rearranges cleanly in solution to an, as yet, unidentified new compound exhibiting a $^{31}\text{P}\{^1\text{H}\}$ NMR resonance at 3.5 ppm. With the ligands **1e** and **1f** the formation of $[\text{Mo}(\text{PNP})(\text{CO})_3]$ complexes was not observed, but the same rearrangement product as in the case of **4c** was detected by $^{31}\text{P}\{^1\text{H}\}$ NMR spectroscopy, giving rise to signals at 14.2 and 5.3 ppm, respectively. Complexes **4–6** were fully characterized by a combination of ^1H , $^{13}\text{C}\{^1\text{H}\}$, and $^{31}\text{P}\{^1\text{H}\}$ NMR spectroscopy, IR spectroscopy, and elemental analysis.

Characteristic features of **4**, **5**, and **6** comprise, in the $^{13}\text{C}\{^1\text{H}\}$ NMR spectrum, low-field triplet resonances in the range 223–231 ppm and 206–216 ppm assignable to the carbonyl carbon atoms *trans* and *cis* to the pyridine nitrogen, respectively. The $^{31}\text{P}\{^1\text{H}\}$ NMR spectra exhibit singlet resonances at 131.9, 148.8, 207.7, 129.3, and 103.3 ppm. The IR spectra show three strong to medium absorption bands in the range 1988 to 1811 cm^{-1} as expected for a meridional arrangement of the three carbonyl ligands.

In addition to the spectroscopic characterization, the solid-state structures of **4a** and **4b** were determined by single-crystal X-ray diffraction. ORTEP diagrams are depicted in Figures 1 and 2 with selected bond distances given in the captions. The coordination geometry around the molybdenum center corresponds to a distorted octahedron. The P(1)–Mo–P(2) angles in the complexes $[\text{Mo}(\text{PNP-Ph})(\text{CO})_3]$,¹³ **4a**, and **4b** are hardly affected by the size of the substituents of the phosphorus atoms, being 155.0(2)°, 155.62(1)°, and 151.73(1)°, respectively. The carbonyl–Mo–carbonyl angles of the CO ligands *trans* to one

(10) Müller, G.; Klinga, M.; Leskelä, M.; Rieger, B. *Z. Anorg. Allg. Chem.* **2002**, 628, 2839.

(11) Ansell, J.; Wills, M. *Chem. Soc. Rev.* **2002**, 31, 259.

(12) For related chiral PCP ligands and complexes see: (a) Gorla, F.; Togni, A.; Venanzi, L. M.; Albinati, A.; Lianza, F. *Organometallics* **1994**, 13, 1607. (b) Longmire, J. M.; Zhang, X.; Shang, M. *Organometallics* **1998**, 17, 4374. (c) Longmire, J. M.; Zhang, X. *Tetrahedron Lett.* **1997**, 38, 1725. (d) Williams, B. S.; Dani, P.; Lutz, M.; Spek, A. L.; van Koten, G. *Helv. Chim. Acta* **2001**, 84, 3519. (e) Albrecht, M.; Kocks, B. M.; Spek, A. L.; van Koten, G. *J. Organomet. Chem.* **2001**, 624, 271.

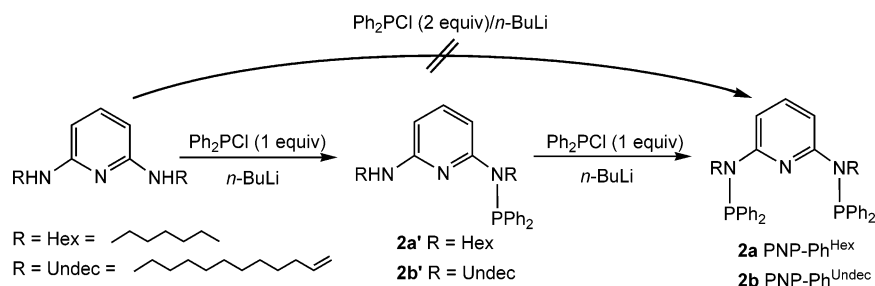
(13) (a) Schirmer, W.; Flörke, U.; Haupt, H.-J. *Z. Anorg. Allg. Chem.* **1987**, 545, 83. (b) Schirmer, W.; Flörke, U.; Haupt, H.-J. *Z. Anorg. Allg. Chem.* **1989**, 574, 239.

(14) Aime, S.; Harris, R. K.; McVicker, E. M.; Fild, M. *J. Chem. Soc., Dalton Trans.* **1976**, 2144.

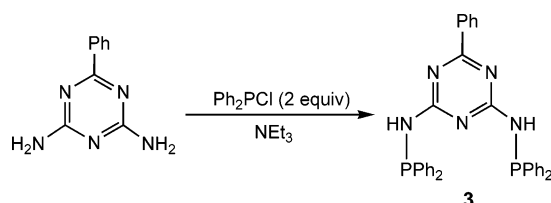
(15) Hunter, D.; Michie, J. K.; Miller, J. A.; Stewart, W. *Phosphorus Sulfur* **1981**, 10, 267.

(16) (a) Lang, H.-F.; Fanwick, P. E.; Walton, R. A. *Inorg. Chim. Acta* **2002**, 392, 1.

Scheme 2



Scheme 3



another, on the other hand, viz., C(1)–Mo–C(2), C(19)–Mo–C(20), and C(23)–Mo–C(24), vary strongly with the bulkiness of the PR₂ moiety (PPh₂ < PPr^t₂ < PBu^t₂) and decrease from 171.1(8)° in [Mo(PNP-Ph)(CO)₃] to 166.03(5)° in **4a**, and finally to 156.53(4)° in **4b**.

As part of our interest in the chemistry of molybdenum PNP complexes, we have begun to investigate the reactivity of complexes **4** and **5** toward iodine. In fact, complexes **4a** and **5** react readily with 1 equiv of I₂ in CH₂Cl₂ to afford the seven-

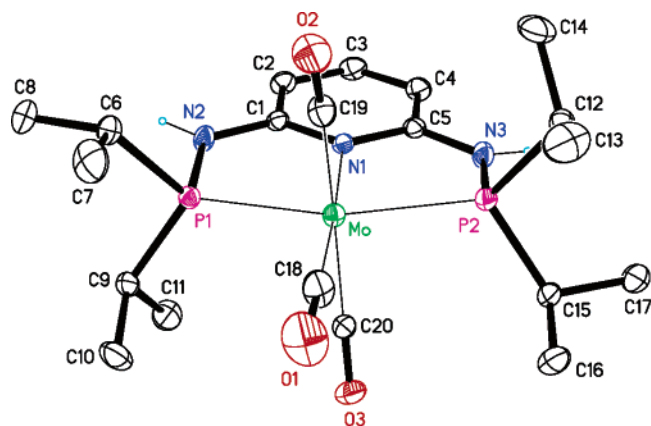


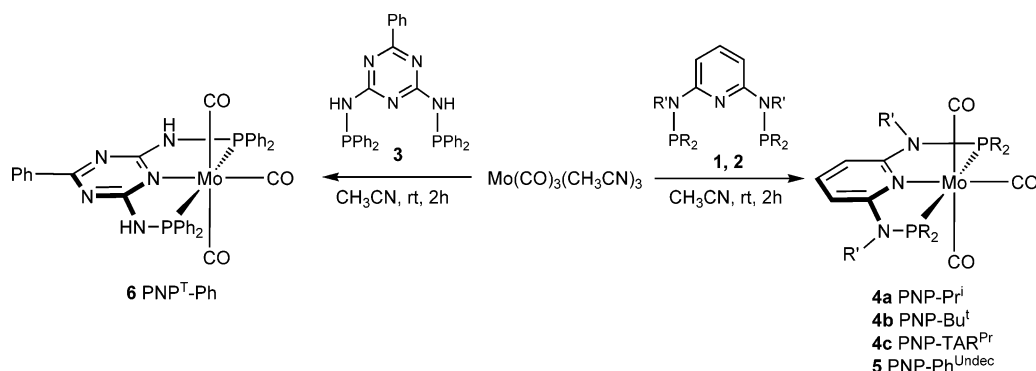
Figure 1. Structural view of Mo(PNP-Pr^t)(CO)₃·CH₃CN (**4a**·CH₃CN) showing 30% thermal ellipsoids (C-bonded H atoms and CH₃CN omitted for clarity). Selected bond lengths (Å) and bond angles (deg): Mo–C(18) 1.948(1), Mo–C(19) 2.001(2), Mo–C(20) 2.024(1), Mo–N(1) 2.251(1), Mo–P(1) 2.4206(3), Mo–P(2) 2.3986(3); P(1)–Mo–P(2) 155.62(1), C(19)–Mo–C(20) 166.03(5).

coordinate complexes [Mo(PNP-Pr^t)(CO)₃]I (**7a**) and [Mo(PNP-Ph^{Undec})(CO)₃]I (**7c**), respectively (Scheme 5). Noteworthy, treatment of **4a** with 2 equiv of I₂ results in the formation of [Mo(PNP-Pr^t)(CO)₃]I₃ (**7b**), which differs from **7a** only by the nature of the counterion, i.e., triiodide versus iodide. On the other hand, if the reaction of **4a** and I₂ is carried out in CH₃CN instead of CH₂Cl₂, the mono-acetonitrile complex [Mo(PNP-Pr^t)(CO)₂(CH₃CN)]I (**8**) is obtained. The identity of compounds **7** and **8** was established by ¹H and ³¹P{¹H} NMR spectroscopy, IR spectroscopy, and elemental analysis. **7c** was also characterized by ¹³C{¹H} NMR spectroscopy. In addition, the solid-state structures of **7b** and **8** have been determined by X-ray crystallography. According to our knowledge, **7** and **8** are the first seven-coordinate pincer molybdenum complexes.

Seven-coordinate complexes are notorious for their fluxional behavior in solution.^{17,18} None of the idealized geometries, capped prism, capped octahedron, and pentagonal bipyramid, nor any of less symmetrical arrangements are characterized by a markedly lower total energy.¹⁹ Hence, interconversions between these various structures are quite facile. Thus, as expected, the ³¹P{¹H} NMR spectra of **7a**, **7c**, and **8** exhibit only one resonance at 114.0, 127.8, and 113.8 ppm at room temperature and even at –90 °C in CD₂Cl₂ as the solvent. The ¹³C{¹H} NMR spectrum of **7c** shows two low-field triplet carbonyl resonances (2:1 ratio) centered at 255.0 and 227.8 ppm. Complexes **7** and **8** both display three ν_{CO} bands in the solid-state IR spectra. In addition, the nitrile ligand in **8** gives rise to two nitrile resonances at 2299 and 2269 cm⁻¹. Detailed investigations concerning the dynamics of this type of complexes are in progress and will be reported in due course.

Molecular views of **7b** and **8** are depicted in Figures 3 and 5, with selected bond distances and angles reported in the captions. The coordination geometry around the molybdenum center may be viewed as a distorted capped trigonal prism. This is emphasized in Figure 4, showing a view of the inner coordination sphere of **7b** and **8** with N(1) capping the quadrilateral face. The angles used to describe an ideal capped trigonal prism in which all M–L distances are equal are shown in Chart 1. L_c

Scheme 4



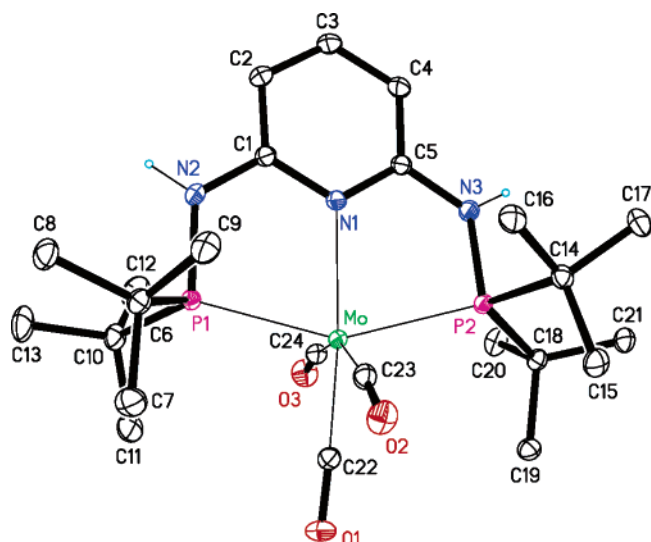
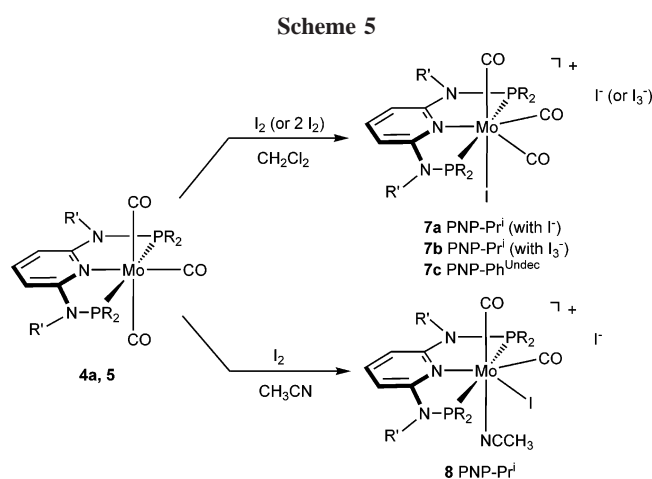


Figure 2. Structural view of $\text{Mo}(\text{PNP-Bu}^t)(\text{CO})_3 \cdot \text{CH}_3\text{CN}$ (**4b**· CH_3CN) showing 40% thermal ellipsoids (C-bonded H atoms and CH_3CN omitted for clarity). Selected bond lengths (Å) and bond angles (deg): Mo–C(22) 1.924(1), Mo–C(23) 2.011(1), Mo–C(24) 2.008(1), Mo–N(1) 2.284(1), Mo–P(1) 2.4638(3), Mo–P(2) 2.4767(3); P(1)–Mo–P(2) 151.73(1), C(23)–Mo–C(24) 156.53(4).



(N1) is the capping ligand, L_f are ligands in the capped rectangular face, and L_e are the ligands in the unique edge of the capped prism. In the ideal case Θ_1 and Θ_2 are 82° and 148° , respectively. In the case at hand, Θ_1 and Θ_2 are taken as average values of the four L_c –Mo– L_f and the two L_c –Mo– L_e angles. For **7b** and **8** these angles are 80.1° and 144.4° and 79.1° and 145.6° , respectively.

Iron PNP Pincer Complexes. With the exception of the bulky PNP-Bu^t (**1c**), the reaction of $[\text{Fe}(\text{H}_2\text{O})_6](\text{BF}_4)_2$ with 1 equiv of **1a–h**, **2a**, **2b**, and **3**, respectively, in acetonitrile at room temperature for 2 h affords on workup the air-stable diamagnetic trisacetonitrile complexes $[\text{Fe}(\text{PNP})(\text{CH}_3\text{CN})_3](\text{BF}_4)_2$ (**9a–f**), $[\text{Fe}(\text{PNP-Ph}^{\text{Undec}})(\text{CH}_3\text{CN})_3](\text{BF}_4)_2$ (**10a**), $[\text{Fe}(\text{PNP-Ph}^{\text{Hex}})(\text{CH}_3\text{CN})_3](\text{BF}_4)_2$ (**10b**), and $[\text{Fe}(\text{PNP}^t\text{-Ph})(\text{CH}_3\text{CN})_3](\text{BF}_4)_2$ (**11**) in high isolated yields (Scheme 6). In the case of PNP-Bu^t only intractable materials were obtained. It is

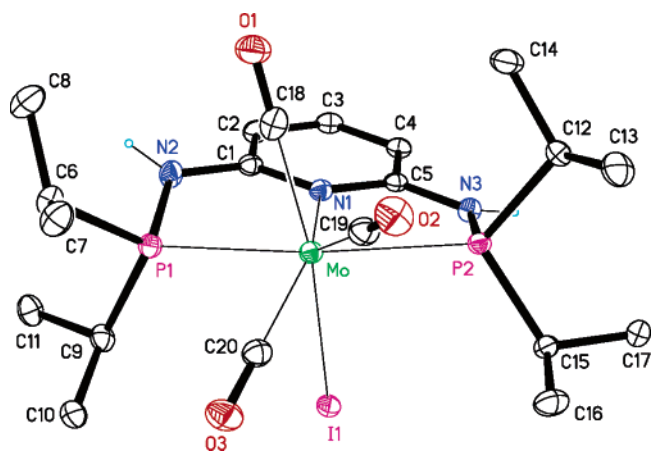


Figure 3. Structural view of $[\text{Mo}(\text{PNP-Pr}^t)(\text{CO})_3]\text{I}_3$ (**7b**) showing 40% thermal ellipsoids (C-bonded H atoms and I_3^- omitted for clarity). Selected bond lengths (Å) and bond angles (deg): Mo–C(18) 2.019(2), Mo–C(19) 1.984(2), Mo–C(20) 2.012(2), Mo–N(1) 2.230(2), Mo–P(1) 2.5211(6), Mo–P(2) 2.5163(6), Mo–I(1) 2.8556(2); P(1)–Mo–P(2) 153.32(2), N(1)–Mo–P(1) 77.33(5), N(1)–Mo–P(2) 76.87(5), N(1)–Mo–C(18) 82.5(1), N(1)–Mo–C(19) 137.4(1), N(1)–Mo–C(20) 151.3(1), N(1)–Mo–I(1) 83.32(4).

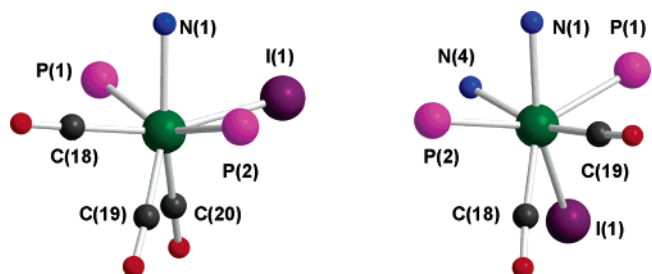


Figure 4. Structural views of the inner coordination sphere of $[\text{Mo}(\text{PNP-Pr}^t)(\text{CO})_3]\text{I}_3^+$ (**7b**) (left) and $[\text{Mo}(\text{PNP-Pr}^t)(\text{CO})_2(\text{CH}_3\text{CN})]\text{I}^+$ (**8**) (right) emphasizing the capped trigonal prism description with N(1) capping the quadrilateral face.

interesting to note that small amounts of water apparently do not cause hydrolysis, resulting in cleavage of P–N and/or P–O bonds of the PNP ligands. All these complexes have been characterized by a combination of elemental analysis and ^1H , $^{13}\text{C}\{^1\text{H}\}$, and $^{31}\text{P}\{^1\text{H}\}$ NMR spectroscopy. In addition, the solid-state structures of $[\text{Fe}(\text{PNP-Ph})(\text{CH}_3\text{CN})_3](\text{BF}_4)_2$ (**9a**), $[\text{Fe}(\text{PNP-Pr}^t)(\text{CH}_3\text{CN})_3](\text{BF}_4)_2$ (**9b**), $[\text{Fe}(\text{PNP-BIPOL})(\text{CH}_3\text{CN})_3](\text{BF}_4)_2$ (**9d**), and the chiral $[\text{Fe}(\text{PNP-TAR}^{\text{Me}})(\text{CH}_3\text{CN})_3](\text{BF}_4)_2$ (**9f**) were determined by single-crystal X-ray diffraction. These complexes all exhibit a singlet resonance in the $^{31}\text{P}\{^1\text{H}\}$ NMR spectrum in the range of about 98 to 194 ppm. In the ^1H NMR spectrum the NH protons give rise to a slightly broadened singlet in the range 7.30 to 8.89 ppm. All other resonances are unremarkable and are not discussed here.

ORTEP diagrams of **9d**, **9f**, and **11** are depicted in Figures 6, 7, and 8 with selected bond distances and angles reported in the captions. ORTEP diagrams of **9a** and **9b** are provided in the Supporting Information. All five complexes adopt a distorted octahedral geometry around the metal center. The PNP ligands are coordinated to the iron center in a tridentate meridional mode, with P–Fe–P angles around 166° . The mean bond lengths around Fe of these compounds are Fe–P 2.218 Å, Fe– N_{py} 1.974 Å, Fe– N_{trans} 1.932, and Fe– N_{cis} 1.917 Å. The Fe–P bond length is systematically longer for aryl-bearing P (mean value 2.245 Å) than for the P–O-bearing phosphines (**9d** and **9f**, mean value 2.191 Å). The Fe–N bonds of the nitriles

(17) Curtis, M. D.; Shiu, K.-B. *Inorg. Chem.* **1985**, *24*, 1213.

(18) Baker, P. K.; Al-Jahdali, M.; Meehan, M. M. *J. Organomet. Chem.* **2002**, *648*, 99. (b) Baker, P. K.; Drew, M. G. B.; Moore, D. S. *J. Organomet. Chem.* **2002**, *663*, 45.

(19) (a) Hoffmann, R.; Beier, B. F.; Muetterties, E. L.; Rossi, A. R. *Inorg. Chem.* **1977**, *16*, 511. (b) Thompson, H. B.; Bartell, L. S. *Inorg. Chem.* **1968**, *7*, 488.

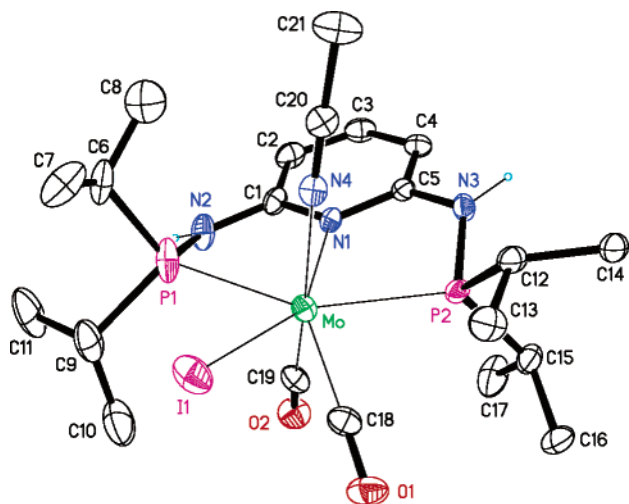
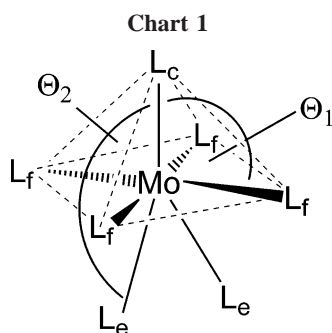


Figure 5. Structural view of $[\text{Mo}(\text{PNP-Pr}^i)(\text{CO})_2(\text{CH}_3\text{CN})\text{I}]\text{I}$ (**8**) showing 40% thermal ellipsoids (C-bonded H atoms and I^- omitted for clarity). Selected bond lengths (Å) and bond angles (deg): Mo–C(18) 1.985(7), Mo–C(19) 1.952(7), Mo–N(1) 2.231(5), Mo–N(4) 2.248(6), Mo–P(1) 2.520(2), Mo–P(2) 2.466(2), Mo–I(1) 2.8649(7); P(1)–Mo–P(2) 150.42(7), N(1)–Mo–C(18) 140.1(2), N(1)–Mo–C(19) 82.8(2), N(1)–Mo–N(4) 82.1(2), N(1)–Mo–P(1) 75.4(1), N(1)–Mo–P(2) 76.1(1), N(1)–Mo–I(1) 151.0(1).



trans to the pyridine nitrogen of the PNP ligand are typically longer than the ones *cis* to the PNP moiety. The aminophosphine nitrogen atoms are typically active hydrogen bond donors, as shown for example in Figure 6. Anions as well as suitable solvent molecules (CH_3CN , Et_2O , H_2O) are comparatively well anchored by this hydrogen bonding.

Attempts to obtain zerovalent iron complexes of the type $[\text{Fe}(\text{PNP})(\text{CH}_3\text{CN})_2]$ by reacting $[\text{Fe}(\text{PNP-BIPOL})(\text{CH}_3\text{CN})_3](\text{BF}_4)_2$ (**9d**) with NaHg (3%) failed. In fact, treatment of **9d** with an excess of NaHg in acetonitrile resulted in the immediate

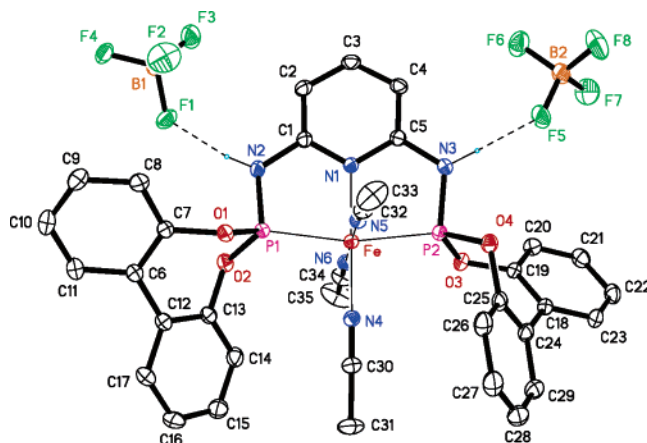
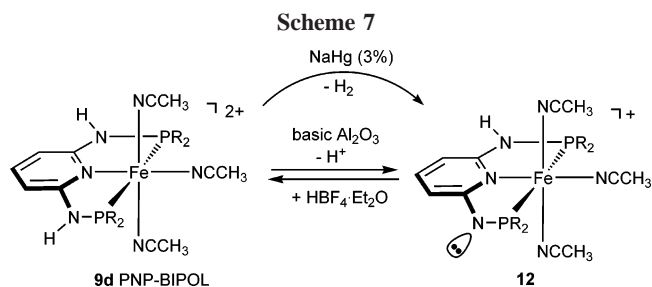
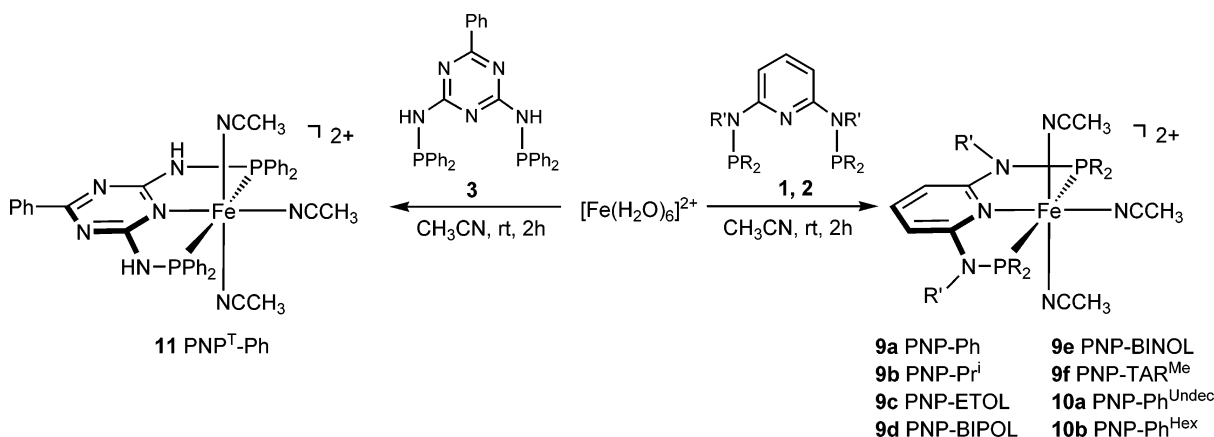


Figure 6. Structural view of $[\text{Fe}(\text{PNP-BIPOL})(\text{CH}_3\text{CN})_3](\text{BF}_4)_2 \cdot \text{solv}$ (**9d**·solv) showing 30% thermal ellipsoids (C-bonded H atoms and second independent complex omitted for clarity). Selected bond lengths (Å) and bond angles (deg): Fe–P(1) 2.1895(5), Fe–P(2) 2.1881(5), Fe–N(1) 1.975(2), Fe–N(4) 1.931(2), Fe–N(5) 1.917(2), Fe–N(6) 1.913(2), P(1)–N(2) 1.658(2), P(2)–N(3) 1.653(2), N(2)–C(1) 1.387(2), N(3)–C(5) 1.389(2); P(1)–Fe–P(2) 165.62(2).



evolution of gas (H_2), affording the deprotonated monocationic complex $[\text{Fe}(\text{PNP-BIPOL})(\text{CH}_3\text{CN})_3]\text{BF}_4$ (**12**) as shown in Scheme 7. Noteworthy, complex **12** was also obtained when **9d** was chromatographed on basic alumina. Thus, in this case the reduction of the metal center is apparently hampered by the acidic NH protons of the PNP ligand. The identity of **12** was unequivocally established by X-ray crystallography. A structural view of **12** is shown in Figure 9, with selected bond distances and angles reported in the caption. The bond lengths involving the deprotonated nitrogen N(2) are significantly shorter than for their hydrogen-bearing counterparts. The ^1H , $^{13}\text{C}\{^1\text{H}\}$, and $^{31}\text{P}\{^1\text{H}\}$ NMR spectra are not very informative, exhibiting only broad and featureless or averaged resonances even at -70°C in $\text{THF-}d_8$. For instance, in the $^{31}\text{P}\{^1\text{H}\}$ NMR

Scheme 6



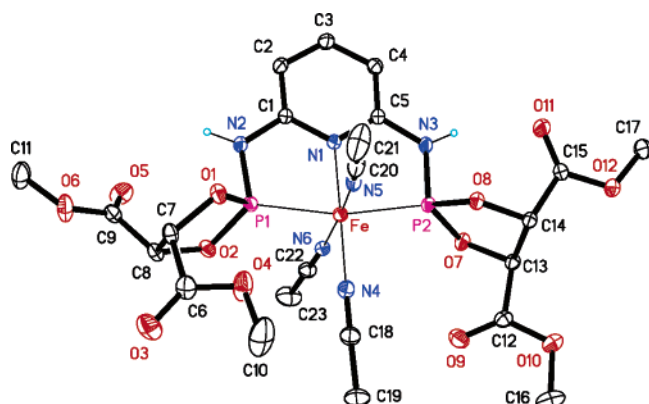


Figure 7. Structural view of $[\text{Fe}(\text{PNP-TAR}^{\text{Me}})(\text{CH}_3\text{CN})_3](\text{BF}_4)_2$ (**9f**) showing 30% thermal ellipsoids (C-bonded H atoms and BF_4^- omitted for clarity). Selected bond lengths (\AA) and bond angles (deg): Fe–P(1) 2.1916(4), Fe–P(2) 2.2134(4), Fe–N(1) 1.976(2), Fe–N(4) 1.930(2), Fe–N(5) 1.919(2), Fe–N(6) 1.930(2), P(1)–N(2) 1.661(2), P(2)–N(3) 1.673(2), N(2)–C(1) 1.387(2), N(3)–C(5) 1.382(2); P(1)–Fe–P(2) 166.74(2).

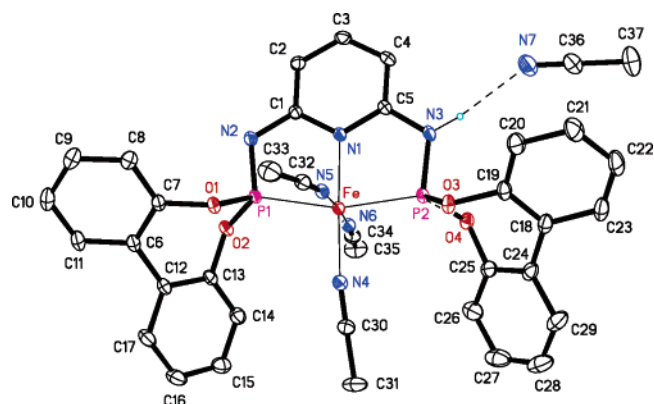


Figure 9. Structural view of $[\text{Fe}(\text{PNP-BIPOL})(\text{CH}_3\text{CN})_3]\text{BF}_4 \cdot \text{CH}_3\text{CN}$ (**12**· CH_3CN) showing 30% thermal ellipsoids (C-bonded H atoms and BF_4^- omitted for clarity). Selected bond lengths (\AA) and bond angles (deg): Fe–P(1) 2.2114(4), Fe–P(2) 2.1736(4), Fe–N(1) 1.982(1), Fe–N(4) 1.931(1), Fe–N(5) 1.910(1), Fe–N(6) 1.927(1), P(1)–N(2) 1.614(1), P(2)–N(3) 1.656(1), N(2)–C(1) 1.362(2), N(3)–C(5) 1.392(2); P(1)–Fe–P(2) 163.30(2).

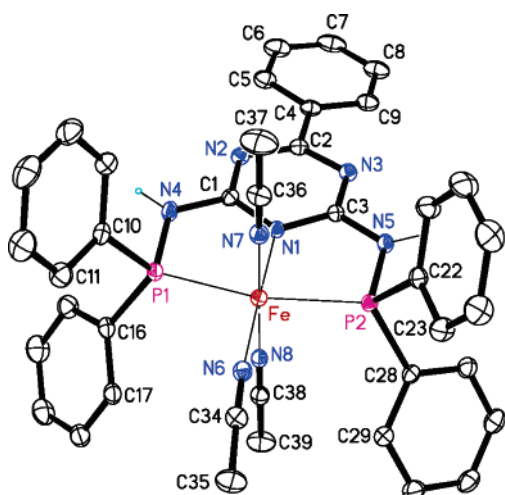
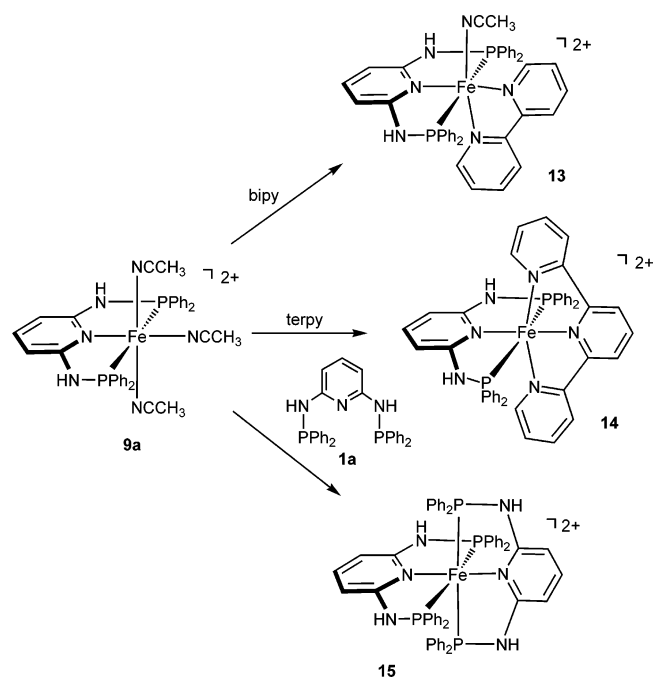


Figure 8. Structural view of $[\text{Fe}(\text{PNP}^t\text{-Ph})(\text{CH}_3\text{CN})_3](\text{BF}_4)_2 \cdot 3\text{ClCH}_2\text{CH}_2\text{Cl} \cdot \text{H}_2\text{O}$ (**11**· $3\text{ClCH}_2\text{CH}_2\text{Cl} \cdot \text{H}_2\text{O}$) showing 40% thermal ellipsoids (C-bonded H atoms, BF_4^- and solvent molecules omitted for clarity). Selected bond lengths (\AA) and bond angles (deg): Fe–P(1) 2.2430(4), Fe–P(2) 2.2409(4), Fe–N(1) 1.957(1), Fe–N(6) 1.942(1), Fe–N(7) 1.914(1), Fe–N(8) 1.915(1), P(1)–N(4) 1.707(1), P(2)–N(5) 1.702(1), N(4)–C(1) 1.355(2), N(5)–C(3) 1.353(2); P(1)–Fe–P(2) 165.44(2).

spectrum a singlet at 194.38 ppm is observed (cf. 186.67 ppm for **9d**). This may be attributed to a fast proton exchange process between the two N-sites. The deprotonation of $[\text{Fe}(\text{PNP-BIPOL})(\text{CH}_3\text{CN})_3](\text{BF}_4)_2$ (**9d**) is reversible, and addition of 1 equiv of $\text{HBF}_4 \cdot \text{OEt}_2$ to a solution of **12** in CD_3CN cleanly yields **9d** as monitored by ^1H and $^{31}\text{P}\{^1\text{H}\}$ NMR spectroscopy.

The nitrile ligands in complexes **9**, **10**, and **11** are substitutionally labile and are readily replaced by other nitrogen donor ligands. The substitution chemistry of $[\text{Fe}(\text{PNP})(\text{CH}_3\text{CN})_3]^{2+}$ has been exemplarily investigated with **9a** as model complex. Treatment of **9a** with bipyridine, terpyridine, and PNP-Ph (**1a**) yields the formation of complexes **13**–**15**, respectively, in high isolated yields (Scheme 8). Alternatively, **15** can be obtained directly by reacting $[\text{Fe}(\text{H}_2\text{O})_6](\text{BF}_4)_2$ with 2 equiv of **1a** in THF as the solvent. Structural views of **13** and **14** are given in Figures 10 and 11 (a structural view of **15** is given in the Supporting Information). Selected bond distances and angles are reported in the captions.

Scheme 8



Ruthenium PNP Pincer Complexes. The dichloride complexes $\text{Ru}(\text{PNP})(\text{PPh}_3)\text{Cl}_2$ (**16**) are conveniently prepared by a ligand exchange reaction of $\text{RuCl}_2(\text{PPh}_3)_3$ with a stoichiometric amount of the respective PNP ligands **1a**–**f** in CH_2Cl_2 (Scheme 9). Only in the case of PNP-Bu^t (**1c**) were all attempts to prepare $[\text{Ru}(\text{PNP-Bu}^t)(\text{PPh}_3)\text{Cl}_2]$ unsuccessful. Complexes **16** are yellow to brown solids, stable in both the solid state and in oxygen-free solutions. The retention of one PPh_3 ligand in **16** is clearly shown by elemental analysis and NMR spectroscopy. Due to the rigidity of the $-\text{NHPR}_2$ substituents, the octahedral complexes form only two *mer*-stereoisomers with either a *trans*-dichloro or a *cis*-dichloro arrangement. Mixtures of both of them were not observed. The ^1H , $^{13}\text{C}\{^1\text{H}\}$, and $^{31}\text{P}\{^1\text{H}\}$ NMR spectra of **16** show a single resonance pattern at all temperatures for all nuclei, indicating the presence of a single stereoisomer in solution. Moreover, the $^{31}\text{P}\{^1\text{H}\}$ NMR shows one triplet resonance for PPh_3 centered at 38.2 ($J_{\text{PP}} = 27.7$ Hz) and 38.5 ppm ($J_{\text{PP}} = 24.7$ Hz) for **16a** and **16b**, respectively. In the case of the **16c**–**f** the PPh_3 resonance is slightly downfield shifted,

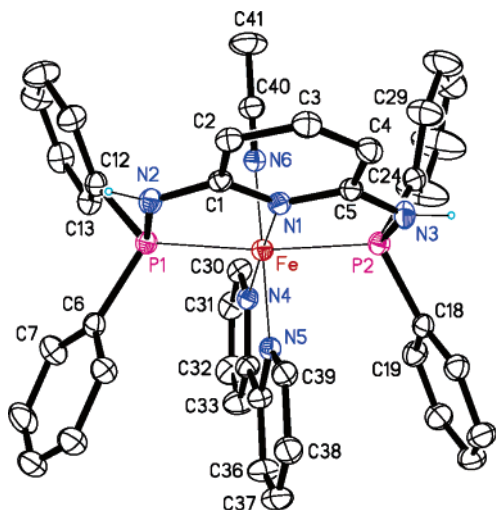


Figure 10. Structural view of $[\text{Fe}(\text{PNP-Ph})(\text{bipy})(\text{CH}_3\text{CN})]\text{BF}_4 \cdot \text{solv}$ (**13**·solv) showing 20% thermal ellipsoids (C-bonded H atoms and BF_4^- omitted for clarity). Selected bond lengths (Å) and bond angles (deg): Fe–P(1) 2.2323(8), Fe–P(2) 2.2274(8), Fe–N(1) 1.978(2), Fe–N(4) 1.958(2), Fe–N(5) 1.960(2), Fe–N(6) 1.908(2); P(1)–Fe–P(2) 167.60(3).

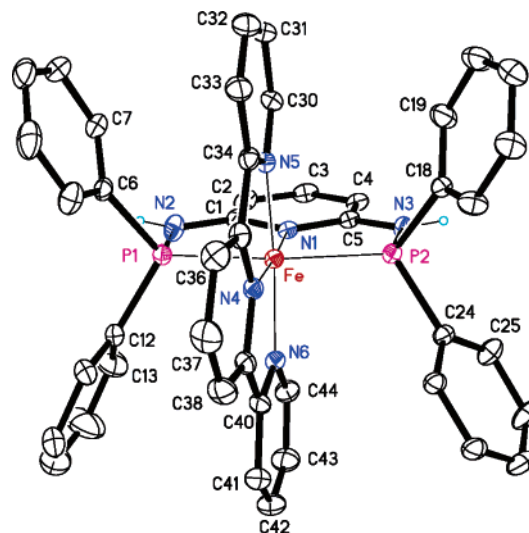


Figure 11. Structural view of $[\text{Fe}(\text{PNP-Ph})(\text{terpy})]\text{BF}_4 \cdot \text{solv}$ (**14**·solv) showing 30% thermal ellipsoids (H atoms and BF_4^- omitted for clarity). Selected bond lengths (Å) and bond angles (deg): Fe–P(1) 2.2361(9), Fe–P(2) 2.2401(9), Fe–N(1) 1.989(2), Fe–N(4) 1.878(3), Fe–N(5) 1.968(3), Fe–N(6) 1.967(3), P(1)–Fe–P(2) 165.97(4).

giving rise to triplets or doublets of doublets centered at 49.0, 45.3, 43.3, and 43.8 ppm, respectively. The J_{PP} coupling constants are significantly larger in the latter case, being in the range 46.2 to 47.8 Hz. The chemical shifts for PPh_3 are typical for being coordinated *trans* to neutral or anionic donor ligands. Accordingly, it is difficult to distinguish whether PPh_3 lies *cis* or *trans* to the pyridine nitrogen. It has to be noted that in analogous ruthenium PNP and also NNN pincer complexes both arrangements have been observed. For instance, in $[\text{RuCl}_2(\text{PNP})(\text{PPh}_3)]$ (PNP = 2,6-bis[(diphenylphosphino)methyl]pyridine),^{5d} $[\text{RuCl}_2(\text{terpy})(\text{PPh}_3)]$,²⁰ and $[\text{RuCl}_2(\text{NNN})(\text{PPh}_3)]$ (NNN = 2,6-bis[(dimethylamino)methyl]pyridine)^{4c} the triphenylphosphine ligand coordinates *trans* to the pyridine nitrogen, the two chlorides lying mutually *trans*, while in $[\text{RuCl}_2(\text{pybox})(\text{PPh}_3)]$ (pybox = 2,6-bis(oxazolonyl)pyridine) PPh_3 is coordinated *cis* to the pyridine nitrogen and the chloride ligands consequently adopt a *cis* configuration.²¹

With the compounds at hand, the ligand arrangement around the metal center of the $[\text{Ru}(\text{PNP})(\text{PPh}_3)\text{Cl}_2]$ complexes could not be assigned unequivocally since all attempts to crystallize a series of complexes **16** were as yet unsuccessful. Only the structure of **16d** could be determined by X-ray crystallography. A structural view of **16d** is depicted in Figure 12, with selected bond distances and angles given in the caption. The geometry around ruthenium can be described as a distorted octahedron

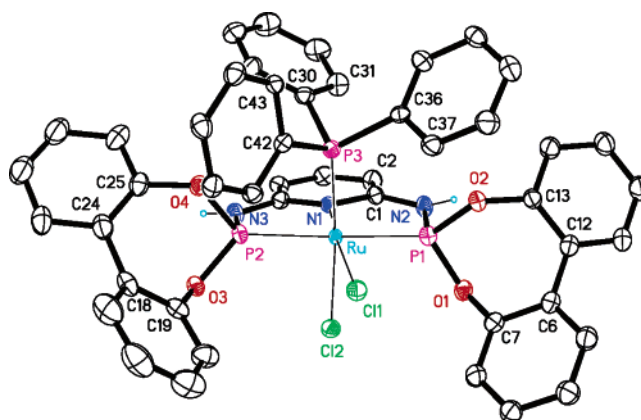
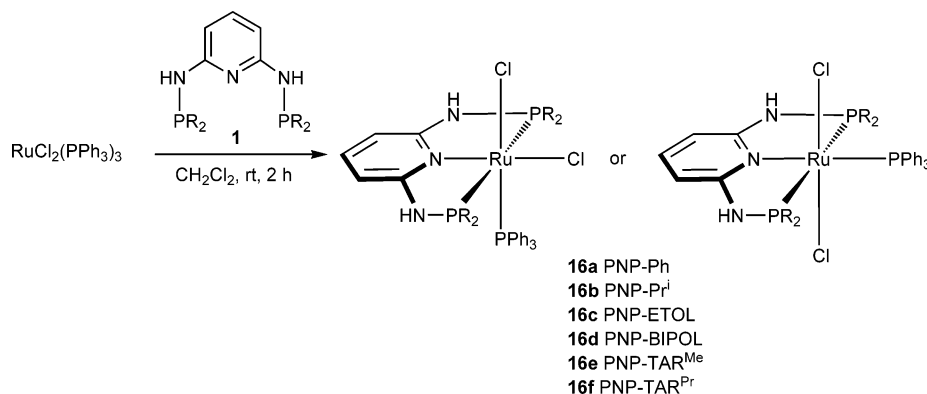


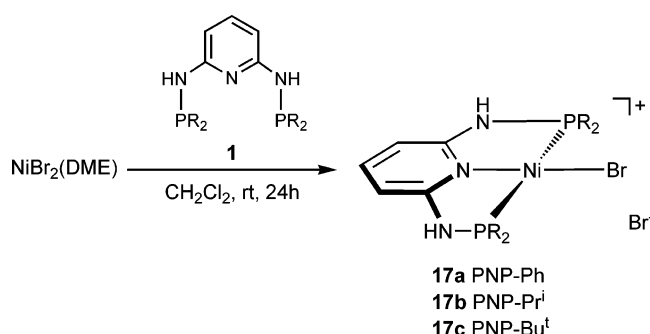
Figure 12. Structural view of *cis*- $\text{Ru}(\text{PNP-BIPOL})(\text{PPh}_3)\text{Cl}_2 \cdot 2\text{CH}_2\text{Cl}_2$ (**16d**· $2\text{CH}_2\text{Cl}_2$) showing 30% thermal ellipsoids (C-bonded H atoms and CH_2Cl_2 omitted for clarity). Selected bond lengths (Å) and bond angles (deg): Ru–P(1) 2.257(3), Ru–P(2) 2.272(3), Ru–N(1) 2.094(7), Ru–P(3) 2.293(2), Ru–Cl(1) 2.431(3), Ru–Cl(2) 2.463(3); P(1)–Ru–P(2) 161.3(1), N(1)–Ru–Cl(1) 170.0(2), N(1)–Ru–Cl(2) 85.8(2), Cl(1)–Ru–Cl(2) 86.9(1).

with a meridional PNP ligand, a PPh_3 ligand *cis* to the pyridine nitrogen atom, and surprisingly two mutually *cis* Cl atoms. The Ru–P(1), Ru–P(2), and Ru–P(3) distances are 2.257-

Scheme 9



Scheme 10



(3), and 2.293(2) Å and are significantly shorter than those in *trans*-[RuCl₂(PNP)(PPh₃)] (PNP = 2,6-bis[(diphenylphosphino)methyl]pyridine) (2.3862(7), 2.3641(7), and 2.3641(7) Å).^{5d} This trend is reversed for the Ru–N(1), Ru–Cl(1), and Ru–Cl(2) bond distances, which are 2.094(7), 2.431(3), and 2.463(3) Å (cf. 2.168(2), 2.4122(7), and 2.4263(7) Å in *trans*-[RuCl₂(PNP)(PPh₃)]). The P(1)–Ru–P(2) angle in **16d** is 161.3(1)° but slightly smaller in *trans*-[RuCl₂(PNP)(PPh₃)], being 157.90(3)°.

Nickel, Palladium, and Platinum PNP Pincer Complexes.

The cationic PNP complexes of Ni(II) [Ni(PNP-Ph)Br]Br (**17a**), [Ni(PNP-Prⁱ)Br]Br (**17b**), and [Ni(PNP-Bu^t)Br]Br (**17c**) were readily prepared by the reaction of NiBr₂(DME) with the ligands **1a–c** in 72 and 94% isolated yields (Scheme 10). Complexes **17** are thermally stable and can be handled in air. Their ³¹P-{¹H} NMR spectra contain a sharp singlet resonance that confirms the equivalence of the phosphorus nuclei in accord with a *trans* geometry. The chemical shifts of these signals are observed at 66.1, 100.6, and 103.7 ppm. The appearance in the ¹³C{¹H} NMR of the characteristic pattern of virtual triplets for the *ipso*-Ph, *i*-Pr, and *t*-Bu carbons in **17a–c** is also consistent with strong coupling of these nuclei to mutually *trans* phosphorus nuclei.

The X-ray crystal structure of **17c** is shown in Figure 13 (a structural view of **17a** is given in the Supporting Information). The Ni center adopts a distorted square-planar geometry defined by two phosphorus atoms, the central nitrogen atom of the PNP ligand, and a bromide atom. The coordination figure shows a notable twist, with P(1) deviating by about 0.3 Å from the meridional main plane because of packing effects. All Ni–P bond lengths lie within the expected range for a *trans*-P–Ni–P arrangement. The Ni–N(1) distance is 1.894(1) Å.

Treatment of [Pd(COD)Cl₂] with the ligands **1a–c**, **2a**, **2b**, and **3** in CH₂Cl₂ for 2 h afforded complexes [Pd(PNP-Ph)Cl]-

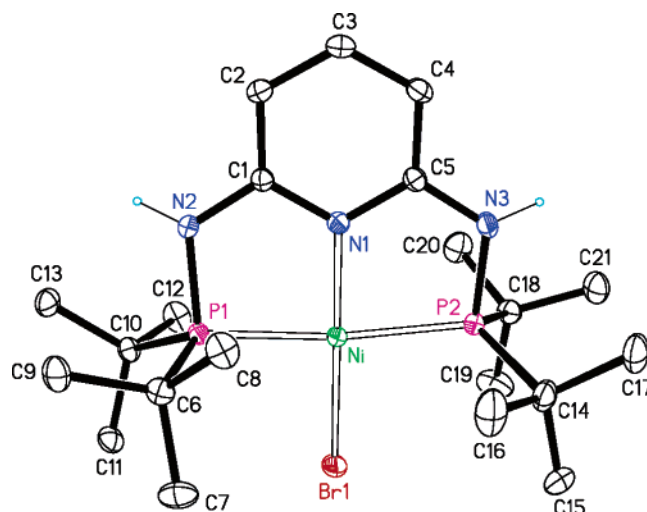
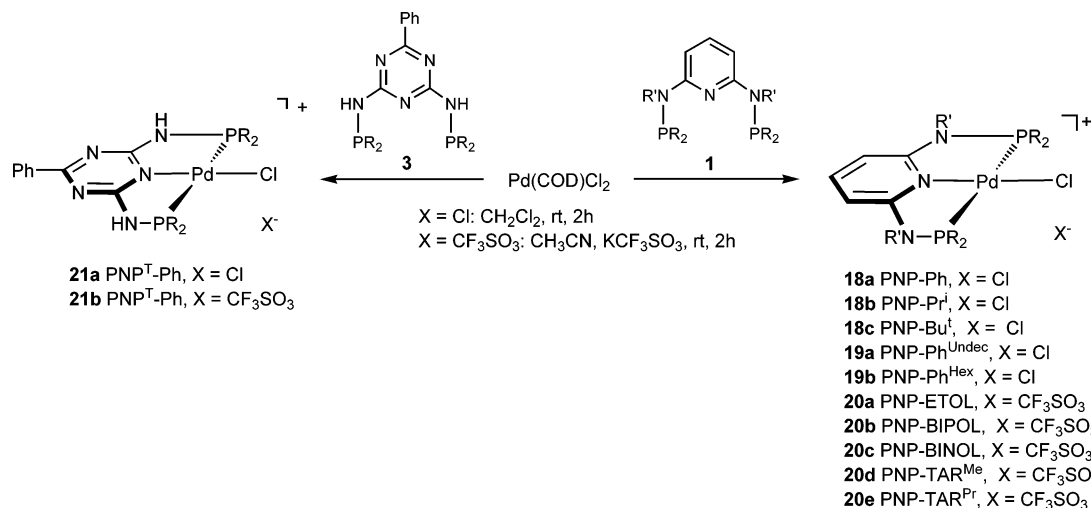


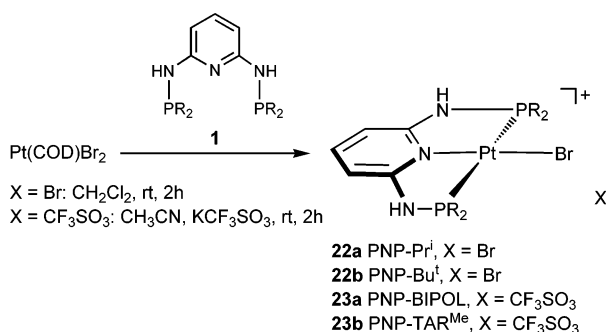
Figure 13. Structural view of [Ni(PNP-Bu^t)Br]Br·0.5CH₃OH (**17c**·0.5CH₃OH) showing 50% thermal ellipsoids (C-bonded H atoms, CH₃OH, and Br⁻ omitted for clarity). Selected bond lengths (Å) and bond angles (deg): Ni–P(1) 2.2067(4), Ni–P(2) 2.2062(4), Ni–N(1) 1.894(1), Ni–Br(1) 2.2987(2); P(1)–Ni–P(2) 169.73(2).

Cl (**18a**), [Pd(PNP-Prⁱ)Cl]Cl (**18b**), [Pd(PNP-Bu^t)Br]Cl, [Pd(PNP-Ph^{Undec})Br]Cl (**19a**), [Pd(PNP-Ph^{Hex})Br]Cl (**19b**), and [Pd(PNP^T-Bu^t)Br]Cl (**21b**) cleanly in good isolated yields (Scheme 11). With ligands **1d–h** the respective palladium complexes turned out to be poorly soluble in most common organic solvents. This could be circumvented by performing the same reaction in the presence of 1 equiv of the halide scavenger KCF₃SO₃ in CH₃CN as the solvent. Accordingly, with the ligands **1d–h** and **3** the complexes [Pd(PNP-ETOL)Cl]CF₃SO₃ (**20a**), [Pd(PNP-BIPOL)Cl]CF₃SO₃ (**20b**), [Pd(PNP-BINOL)Cl]CF₃SO₃ (**20c**), [Pd(PNP-TAR^{Me})Cl]CF₃SO₃ (**20d**), [Pd(PNP-TAR^{Pr})Cl]CF₃SO₃ (**20e**), and [Pd(PNP^T-Ph)Cl]CF₃SO₃ (**21b**) were obtained, which exhibit very good solubility in most organic solvents. Analogous platinum PNP complexes have been prepared in the same manner by reacting [Pt(COD)Br₂] with 1 equiv of ligands **1b**, **1c**, **1e**, and **1g** to yield the platinum complexes **22** and **23** in high yields (Scheme 12). All palladium and platinum PNP complexes are thermally robust off-white to yellow solids that are stable to air both in the solid state and in solution. The identity of the compounds was established by ¹H, ¹³C{¹H}, and ³¹P{¹H} NMR spectroscopy and by elemental

Scheme 11



Scheme 12



analysis. The multinuclear NMR spectra of **18–23** bear no unusual features and are not discussed here.

The identity of **18c** and **20b** was unequivocally established by X-ray crystallography. Structural views of **18c** and **20b** are depicted in Figures 14 and 15, with selected geometric data reported in the captions. The molecules display the usual square-planar coordination around the palladium center. Like in the iron complexes Pd–P bonds to arene bearing phosphorus (**18c**·

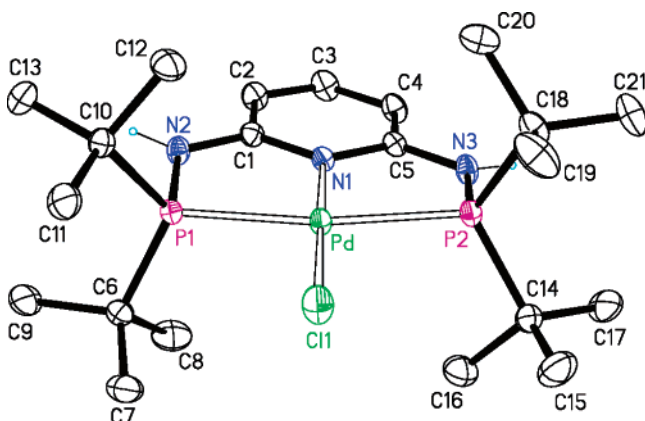


Figure 14. Structural view of $[\text{Pd}(\text{PNP-Bu}^t)\text{Cl}]\text{Cl}\cdot 2\text{CH}_2\text{Cl}_2$ (**18c**· $2\text{CH}_2\text{Cl}_2$) showing 30% thermal ellipsoids (C-bonded H atoms, CH_2Cl_2 , and Cl^- omitted for clarity). Selected bond lengths (Å) and bond angles (deg): Pd–P(1) 2.2987(5), Pd–P(2) 2.2985(5), Pd–N(1) 2.015(2), Pd–Cl(1) 2.3002(6), P(1)–Pd–P(2) 166.54(2).

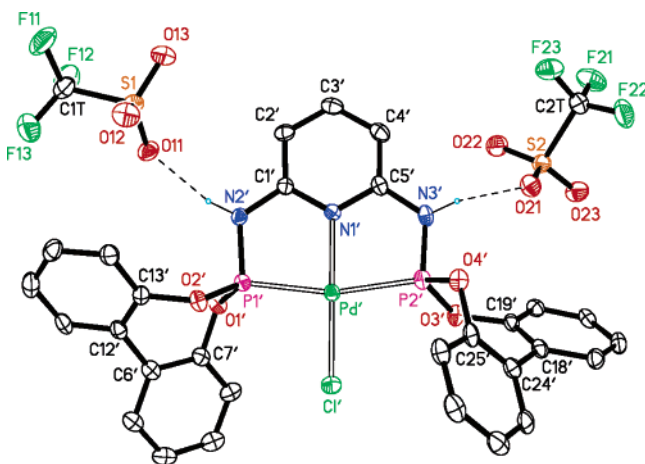
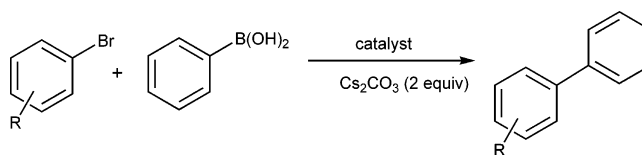


Figure 15. Structural view of $[\text{Pd}(\text{PNP-BIPOL})\text{Cl}]\text{CF}_3\text{SO}_3\cdot (\text{C}_2\text{H}_5)_2\text{O}\cdot 2\text{CH}_3\text{CN}$ (**20b**· $(\text{C}_2\text{H}_5)_2\text{O}\cdot 2\text{CH}_3\text{CN}$) showing 50% thermal ellipsoids (C-bonded H atoms, second independent complex, and solvent molecules omitted for clarity). Selected bond lengths (Å) and bond angles (deg): Pd–P(1) 2.251(2), Pd–P(2) 2.252(2), Pd–N(1) 2.028(4), Pd–Cl 2.271(2), P(1)–Pd–P(2) 165.27(5).

Table 1. Yields of the Suzuki–Miyaura Cross-Coupling of Aryl and Alkyl Bromides with Phenyl Boronic Acid Catalyzed by $[\text{Pd}(\text{PNP-Ph})\text{Cl}]\text{Cl}$ (**18a**), $[\text{Pd}(\text{PNP-Pr}^i)\text{Cl}]\text{Cl}$ (**18b**), and $[\text{Pd}(\text{PNP-Bu}^t)\text{Cl}]\text{Cl}$ (**18c**)^a



entry	R	catalyst (mol %)	yield (%)
1	4-bromotoluene	18a (2)	91
2	4-bromotoluene	18b (2)	90 ^b
3	4-bromotoluene	18c (2)	60 ^b
4	4-bromoacetophenone	18a (2)	98
5	4-bromoacetophenone	18a (0.5)	98 ^b
6	4-bromoacetophenone	18a (0.05)	97 ^b
7	4-bromoanisole	18a (2)	98 ^b
8	4-bromoanisole	18b (2)	93 ^b
9	4-bromoanisole	18a (2)	96
10	4-bromoanisole	18a (0.5)	95 ^b
11	4-bromoanisole	18a (0.05)	87 ^b
12	4-bromonitrobenzene	18a (2)	94
13	2,6-dimethylbromobenzene	18a (2)	66 ^b
14	2,6-dimethylbromobenzene	18a (2)	78
15	1-bromo-2-ethylbenzene	18a (2)	83
16	1-bromododecane	18a (2)	93 ^b
17	2-bromopyridine	18a (2)	94

^a Reaction conditions: 1.0 mmol of bromide, 1.5 mmol of $\text{PhB}(\text{OH})_2$, 2.0 mmol of Cs_2CO_3 , 5 mL of dioxane, 80 °C, 3 h. ^b The reaction was stirred for 16 h.

$2\text{CH}_2\text{Cl}_2$) are about 0.05 Å longer than to oxygen-bearing phosphorus (**20b**· $(\text{C}_2\text{H}_5)_2\text{O}\cdot 2\text{CH}_3\text{CN}$).

Suzuki–Miyaura Coupling. Palladium complexes containing PCP pincer ligands are excellent catalysts for the Suzuki–Miyaura coupling.²² On the basis of these findings we were interested in whether palladium complexes containing PNP ligands exhibit similar reactivities in C–C bond coupling reactions. Accordingly, we investigated the activity of complexes **18a–c** as catalysts for the coupling of various aryl bromides with phenyl boronic acid. The results of this study are summarized in Table 1.

The coupling reaction of 4-bromotoluene with phenylboronic acid catalyzed by **18a–c** proceeded smoothly to give 4-methylbiphenyl in 91, 90, and 60% isolated yields (entries 1–3). This reactivity trend suggests that both the stronger donating ability and the steric demand of the PR_2 substituents make the PNP ligands more electron-rich and renders catalyst **18c** less active. Thus, only **18a** has been utilized as catalyst. The coupling of 4-bromoacetophenone with phenylboronic acid proceeds with 97% isolated yield with a catalyst loading of 0.05 mol % (entry 7), while the electronically deactivated and thus more challenging substrate 4-bromoanisole can be efficiently coupled with 87% isolated yield with a catalyst loading of 0.05 mol % (entry 12). Even the sterically demanding 2,6-dimethylbromobenzene and 1-bromo-2-ethylbenzene gave acceptable yields, viz., 78 and 83% (entries 15 and 16). Attempts to couple 2-bromopyridine and 1-bromododecane, the latter bearing β -hydrogen

(20) Sullivan, B. P.; Calvert, J. M.; Meyer, T. J. *Inorg. Chem.* **1980**, *19*, 1404.

(21) Doberer, D.; Slugovc, C.; Schmid, R.; Kirchner, K.; Mereiter, K. *Monatsh. Chem.* **1999**, *130*, 717.

(22) (a) Miyazaki, F.; Yamaguchi, K.; Shibasaki, M. *Tetrahedron Lett.* **1999**, *40*, 7379. (b) Morales-Morales, D.; Graue, C.; Kasaoka, K.; Redon, R.; Cramer, R. E.; Jensen, C. M. *Inorg. Chim. Acta* **2000**, *300*, 958. (c) Morales-Morales, D.; Redon, R.; Yung, C.; Jensen, C. M. *Chem. Commun.* **2000**, 1619. (d) Bedford, R. B.; Draper, S. M.; Scully, P. N.; Welch, S. L. *New J. Chem.* **2000**, *24*, 745.

atoms, were also successful, resulting in reasonable yields (entries 17 and 18).

It has to be noted that recently evidence was presented that pincer ligands are merely precatalysts, generating some forms of metallic palladium(0), which actually does the catalysis.²³ Pincer ligands possessing only phosphinito donors decomposed even more easily and lead to more active sources of metallic palladium. In the present catalytic reactions we cannot exclude such a possibility.

Concluding Remarks

In sum we have shown that new achiral and chiral PNP ligands are easily prepared from commercially available and inexpensive 2,6-diaminopyridine and 2,6-diamino-4-phenyl-1,3,5-triazine, which can be varied in modular fashion by choosing the appropriate monochloro phosphine or phosphite R₂PCl. These, in turn, are easily accessible in high yields from a large array of both achiral and chiral diols and PCl₃. This methodology contrasts the generally arduous synthetic procedures required for the preparation of 1,3-bis(phosphino)-benzenes. In addition, we showed that *N,N'*-dialkylated diamines such as *N,N'*-di-10-undecenyl-2,6-diaminopyridine and *N,N'*-dihexyl-2,6-diaminopyridine can also be utilized for the synthesis of new PNP ligands. In conjunction with the transition metal fragments [Mo(CO)₃], [Fe(CH₃CN)₃]²⁺, Ru(PPh₃)Cl₂, and MX (M = Ni, Pd, Pt; X = Cl, Br, CF₃COO) stable PNP complexes are formed. For instance, [Mo(CO)₃(CH₃CN)₃] reacts with PNP ligands to give [Mo(PNP)(CO)₃]. Stable octahedral dicationic trisacetonitrile complexes are obtained on treatment of [Fe(H₂O)₆]²⁺ with PNP ligands in CH₃CN. Various *cis* or *trans* dichloro complexes of the type [Ru(PNP)(PPh₃)Cl₂] are afforded via ligand exchange of RuCl₂(PPh₃)₃ with a stoichiometric amount of the respective PNP ligands, and finally [M(PNP)X]Y (M = Ni, Pd, Pt; X = Cl, Br; Y = Cl, Br, CF₃SO₃) complexes are easily accessible from [NiBr₂(DME)] and [M(COD)X₂] (M = Pd, Pt; X = Cl, Br) in the presence or absence of KCF₃SO₃ as halide scavenger. We have also shown that some of these compounds exhibit interesting reactivities leading to novel seven-coordinate pincer complexes in the case of molybdenum or are catalytically active in C–C bond forming reactions such as in the case of palladium. We are currently studying our new PNP ligands in conjunction with other transition metals including Re, Rh, and Ir. Furthermore, the synthetic methodology of obtaining PNP ligands is currently being applied to achiral and chiral PCP ligands based on 1,3-diaminobenzene and derivatives thereof. These studies will be reported in due course.

Experimental Section

General Procedures. All manipulations were performed under an inert atmosphere of argon by using Schlenk techniques. The solvents were purified according to standard procedures. The starting materials PPh₂Cl, PPr₂Cl, PBu₂Cl, and 2,6-diamino-4-phenyl-1,3,5-triazine were purchased from Aldrich and used without further purification. 2-Chloro-1,3,2-dioxaphospholane,²⁴ 2-chlorodibenzo[*d,f*][1,3,2]dioxaphosphine,²⁵ *S*-2-chlorodinaphtho[2,1-*d*:1'2'-*f*][1,3,2]dioxaphosphine,²⁶ 2-chloro-(4*S*,5*S*)-dicarbomethoxy-1,3,2-dioxaphospholane, and 2-chloro-(4*R*,5*R*)-dicarbomethoxy-1,3,2-dioxaphospholane²⁷ were prepared according to the literature.

(23) (a) Sommer, W. J.; Yu, K.; Sears, J. S.; Ji, Y.; Zheng, X.; Davis, R. J.; Sherill, C. D.; Jones, C. W.; Weck, M. *Organometallics* **2005**, *24*, 4351. (b) Eberhard, M. R. *Org. Lett.* **2004**, *6*, 2125.

(24) Lucas, H. J.; Mitchell, F. W., Jr.; Scully, C. N. *J. Am. Chem. Soc.* **1950**, *72*, 5491.

The synthesis of *N,N'*-di-10-undecenyl-2,6-diaminopyridine and *N,N'*-dihexyl-2,6-diaminopyridine is described in the Supporting Information. The deuterated solvents were purchased from Aldrich and dried over 4 Å molecular sieves. ¹H, ¹³C{¹H}, and ³¹P{¹H} NMR spectra were recorded on a Bruker AVANCE-250 spectrometer and were referenced to SiMe₄ and H₃PO₄ (85%), respectively. ¹H and ¹³C{¹H} NMR signal assignments were confirmed by ¹H-COSY, 135-DEPT, and HMQC(¹H–¹³C) experiments.

***N,N'*-Bis(diphenylphosphino)-2,6-diaminopyridine (PNP-Ph) (1a).** This compound was prepared according to the literature.¹³ ¹H NMR (δ, CDCl₃, 20 °C): 7.36–7.34 (m, 2H, Ph, py⁴), 6.54–6.51 (dd, *J* = 7.9 Hz, *J* = 1.6 Hz, 2H, py^{3,5}), 5.39 (s, 2H, NH). ¹³C{¹H} NMR (δ, CDCl₃, 20 °C): 157.6 (d, *J* = 20.2 Hz, py^{2,6}), 139.9 (d, *J* = 12.1 Hz, py⁴), 134.0 (Ph), 131.3 (d, *J* = 20.9 Hz, Ph^{2,6}), 129.2 (Ph⁴), 128.5 (d, *J* = 6.7 Hz, Ph^{3,5}), 99.2 (d, *J* = 14.8 Hz, py^{3,5}). ³¹P{¹H} NMR (δ, CDCl₃, 20 °C): 28.0.

***N,N'*-Bis(diisopropylphosphino)-2,6-diaminopyridine (PNP-Prⁱ) (1b).** To a suspension of 2,6-diaminopyridine (1.8 g, 16.4 mmol) in toluene was added NEt₃ (4.0 mL, 32.8 mmol). The mixture was then cooled to 0 °C, and PPr₂Cl (5.0 g, 32.8 mmol) was added dropwise. Upon further cooling to –70 °C, *n*-BuLi (32.8 mmol, 14.0 mL of a 2.3 M solution in hexane) was slowly added. The solution was allowed to reach room temperature and was then stirred overnight at 80 °C. After that, the solution was filtered and the solvent was removed under vacuum. The remaining yellow oil was recrystallized from toluene/*n*-hexane (1:1). Yield: 4.3 g (78%). Anal. Calcd for C₁₇H₃₃N₃P₂: C, 59.81; H, 9.74; N, 12.31. Found: C, 59.79; H, 9.66; N, 12.10. ¹H NMR (δ, CDCl₃, 20 °C): 7.23 (t, *J* = 8.0 Hz, 1H, py⁴), 6.42 (dd, *J* = 7.8 Hz, *J* = 2.3 Hz, 2H, py^{3,5}), 4.29 (d, *J* = 11.2 Hz, 2H, NH), 1.78–1.67 (m, *J* = 7.0 Hz, *J* = 2.0 Hz, CH(CH₃)₂), 1.08–0.99 (m, 24H, CH(CH₃)₂). ¹³C{¹H} NMR (δ, CDCl₃, 20 °C): 159.5 (d, *J* = 20.3 Hz, py^{2,6}), 139.1 (py⁴), 98.1 (d, *J* = 18.4 Hz, py^{3,5}), 26.3 (d, *J* = 10.7 Hz, CH(CH₃)₂), 18.6 (d, *J* = 19.6 Hz, CH(CH₃)₂), 17.1 (d, *J* = 7.7 Hz, CH(CH₃)₂). ³¹P{¹H} NMR δ, CDCl₃, 20 °C): 49.0.

***N,N'*-Bis(di-*tert*-butylphosphino)-2,6-diaminopyridine (PNP-Bu^t) (1c).** This ligand has been prepared analogously to **1b** with NEt₃ (3.4 mL, 27.6 mmol), 2,6-diaminopyridine (1.5 g, 13.8 mmol), PBu₂Cl (5.0 g, 27.6 mmol), and *n*-BuLi (27.6 mmol, 15.0 mL of a 1.9 M solution in hexane) as the starting materials. Yield: 3.9 g (73%). Anal. Calcd for C₂₁H₄₁N₃P₂: C, 63.45; H, 10.40; N, 10.57. Found: C, 63.37; H, 10.66; N, 10.41. ¹H NMR (δ, CDCl₃, 20 °C): 7.25 (t, *J* = 7.3 Hz, 1H, py⁴), 6.48 (dd, *J* = 8.0 Hz, *J* = 2.5 Hz, 2H, py^{3,5}), 4.64 (d, *J* = 11.2 Hz, 2H, NH), 1.22–1.15 (m, 36H, C(CH₃)₃). ¹³C{¹H} NMR (δ, CDCl₃, 20 °C): 155.1(py^{2,6}), 138.7 (py⁴), 98.2 (d, *J* = 18.5 Hz, py^{3,5}), 29.4 (d, *J* = 13.9 Hz, C(CH₃)₃), 27.8 (d, *J* = 15.0 Hz, C(CH₃)₃). ³¹P{¹H} NMR (δ, CDCl₃, 20 °C): 60.2.

***N,N'*-Bis(1,2-ethandiolphosphino)-2,6-diaminopyridine (PNP-ETOL) (1d).** To a suspension of 2,6-diaminopyridine (0.6 g, 5.6 mmol) in toluene was added NEt₃ (1.6 mL, 11.2 mmol), and the mixture was cooled to 0 °C. Upon addition of 2-chloro-1,3,2-dioxaphospholane (1.4 g, 11.2 mmol) the mixture was stirred at 80 °C overnight, whereupon a white solid precipitated. After removal of insoluble materials by filtration, the solvent was removed under vacuum, affording a yellow oil, which was recrystallized from toluene/*n*-hexane (1:1). Yield: 1.4 g (64%). Anal. Calcd for C₉H₁₃N₃O₄P₂: C, 37.38; H, 4.53; N, 14.53. Found: C, 37.49; H, 4.45; N, 14.56. ¹H NMR (δ, CDCl₃, 20 °C): 7.28 (t, *J* = 7.9 Hz,

(25) (a) Tsarev, V. N.; Kabro, A. A.; Moiseev, S. K.; Kalinin, V. N.; Bondarev, O. G.; Davankov, V. A.; Gavrilov, K. N. *Russ. Chem. Bull., Int. Ed.* **2004**, *53*, 814. (b) van Rooy, A.; Kamer, P. C. J.; van Leeuwen, P. W. N. M.; Goubitz, K.; Fraanje, J.; Veldman, N.; Spek, A. *Organometallics* **1996**, *15*, 835.

(26) Sablong, R.; Newton, C.; Dierkes, P.; Osborn, J. A. *Tetrahedron Lett.* **1996**, *37*, 4933.

(27) Kadyrov, R.; Heller, D.; Selke, R. *Tetrahedron: Asymmetry* **1998**, *9*, 329.

1H, py⁴), 6.29 (d, *J* = 7.9 Hz, 2H, py^{3,5}), 5.70 (s, 2H, NH), 4.20–4.13 (m, 4H, CH₂), 4.01–3.91 (m, 4H, CH₂). ¹³C{¹H} NMR (δ, CDCl₃, 20 °C): 157.0 (py^{2,6}), 139.6 (py⁴), 100.8 (d, *J* = 12.1 Hz, py^{3,5}), 63.7 (CH₂), 63.5 (CH₂). ³¹P{¹H} NMR (δ, CDCl₃, 20 °C): 129.9.

***N,N'*-Bis(dibenzo[*d,f*][1,3,2]dioxaphosphepine)-2,6-diaminopyridine (PNP-BIPOL) (1e).** This ligand has been prepared analogously to **1d** with NEt₃ (1.5 mL, 12.0 mmol), 2,6-diaminopyridine (0.6 g, 6.0 mmol), and 2-chlorodibenzo[*d,f*][1,3,2]dioxaphosphepine (3.0 g, 12.0 mmol) as the starting materials. Yield: 3.4 g (79%). Anal. Calcd for C₂₉H₂₁N₃O₄P₂: C, 64.81; H, 3.94; N, 7.82. Found: C, 64.89; H, 4.06; N, 7.72. ¹H NMR (δ, CDCl₃, 20 °C): 7.50–7.15 (m, 14H, Ph^{3,5} and Ph⁴), 6.40 (d, *J* = 7.8 Hz, 1H, py⁴), 6.11 (dd, *J* = 31.6 Hz, *J* = 7.9 Hz, 2H, Ph^{2,6}), 5.89 (t, *J* = 7.8 Hz, 2H, py^{3,5}), 4.32 (s, 2H, NH). ¹³C{¹H} NMR (δ, CDCl₃, 20 °C): 154.2 (d, *J* = 17.3 Hz, py^{2,6}), 149.5 (d, *J* = 3.8 Hz, Ph), 140.0 (py⁴), 131.6 (d, *J* = 3.1, Ph), 129.8 (Ph), 129.2 (Ph), 125.3 (Ph), 122.3 (Ph), 101.5 (d, *J* = 12.3 Hz, py^{3,5}). ³¹P{¹H} NMR (δ, CDCl₃, 20 °C): 147.5.

***N,N'*-Bis(*S*-dinaphtho[2,1-*d*:1'2'-*f*][1,3,2]dioxaphosphepine)-2,6-diaminopyridine (PNP-BINOL) (S-1f).** A solution of 2,6-diaminopyridine (46 mg, 0.42 mmol) in THF (10 mL) was cooled to –70 °C, and *n*-BuLi (0.85 mmol, 0.47 mL of a 2.10 M solution in hexane) was added. The reaction was stirred until the temperature was –20 °C, and *S*-2-chloro-dinaphtho[2,1-*d*:1'2'-*f*][1,3,2]dioxaphosphepine (300 mg, 0.85 mmol) in 2 mL of THF was added. After allowing the reaction to stir overnight at room temperature, the mixture was filtered, and the solvent removed under vacuum. Yield: 350 mg (94%). Anal. Calcd for C₄₅H₂₉N₃O₄P₂: C, 73.27; H, 3.96; N, 5.70. Found: C, 73.39; H, 3.80; N, 5.52. ¹H NMR (δ, CDCl₃, 20 °C): 8.00–7.85 (m, 8H, Ph), 7.54–7.29 (m, 16H, Ph and py⁴), 6.11–6.02 (m, *J* = 7.9 Hz, *J* = 13.7 Hz, 2H, py^{3,5}), 5.72 (d, *J* = 8.2 Hz, 2H, NH). ¹³C{¹H} NMR (δ, CDCl₃, 20 °C): 162.2 (py^{2,6}), 139.7 (py⁴), 130.4 (Ph), 129.9 (Ph), 129.8 (Ph), 128.5 (Ph), 128.4 (Ph), 126.9 (Ph), 126.7 (Ph), 126.4 (Ph), 126.2 (Ph), 125.0 (Ph); 100.6 (py^{3,5}). ³¹P{¹H} NMR (δ, CDCl₃, 20 °C): 146.1.

***N,N'*-Bis(4*S*,5*S*-dicarbomethoxy-1,3,2-dioxaphospholane)-2,6-diaminopyridine (PNP-TAR^{Me}) (S,S-1g).** This ligand has been prepared analogously to **1d** with NEt₃ (2.3 mL, 16.4 mmol), 2,6-diaminopyridine (0.9 g, 8.2 mmol), and 2-chloro-(4*S*,5*S*)-dicarbomethoxy-1,3,2-dioxaphospholane (4.0 g, 16.4 mmol) as the starting materials. Yield: 1.6 g (66%). Anal. Calcd for C₁₇H₂₁N₃O₁₂P₂: C, 39.17; H, 4.06; N, 8.06. Found: C, 39.19; H, 4.16; N, 7.96. ¹H NMR (δ, CDCl₃, 20 °C): 7.30 (t, *J* = 7.9 Hz, 1H, py⁴) 6.45 (s, 2H, NH), 6.28 (d, *J* = 7.9 Hz, 2H, py^{3,5}), 5.06–5.03 (m, 2H, CH), 4.81–4.75 (m, 2H, CH), 3.83 (s, 6H, CH₃). ¹³C{¹H} NMR (δ, CDCl₃, 20 °C): 171.3 (CO), 169.0 (CO), 153.8 (d, *J* = 14.9 Hz, py^{2,6}), 139.7 (py⁴), 101.9 (d, *J* = 10.3 Hz, py^{3,5}), 77.6 (CH), 77.1 (CH), 76.7 (t, *J* = 10.1 Hz, CH₃), 53.2 (d, *J* = 15.5 Hz, CH₃). ³¹P{¹H} NMR (δ, CDCl₃, 20 °C): 142.9.

***N,N'*-Bis(4*R*,5*R*-dicarboisopropoxy-1,3,2-dioxaphospholane)-2,6-diaminopyridine (PNP-TAR^{Pr}) (R,R-1h).** This ligand has been prepared analogously to **1d** with NEt₃ (2.3 mL, 16.4 mmol), 2,6-diaminopyridine (0.9 g, 8.2 mmol), and 2-chloro-(4*R*,5*R*)-dicarboisopropoxy-1,3,2-dioxaphospholane (5.0 g, 16.4 mmol) as the starting materials. Yield: 5.0 g (95%). Anal. Calcd for C₂₅H₃₇N₃O₁₂P₂: C, 47.40; H, 5.89; N, 6.63. Found: C, 47.50; H, 5.74; N, 6.74. ¹H NMR (δ, CDCl₃, 20 °C): 7.28 (t, *J* = 7.9 Hz, 1H, py⁴) 6.54 (d, *J* = 4.0 Hz, 2H, NH), 6.26 (d, *J* = 7.9 Hz, 2H, py^{3,5}), 5.20–5.06 (m, 4H, (CH₃)₂CH), 4.86–4.84 (m, 2H, CH), 4.62–4.56 (m, 2H, CH), 1.32–1.27 (m, 24H, (CH₃)₂CH). ¹³C{¹H} NMR (δ, CDCl₃, 20 °C): 170.4 (CO), 167.8 (CO), 154.1 (d, *J* = 16.1 Hz, py^{2,6}), 139.6 (py⁴), 101.5 (d, *J* = 10.1 Hz, py^{3,5}), 77.4 (CH), 76.5 (CH), 70.8 ((CH₃)₂CH), 70.2 ((CH₃)₂CH), 21.6 ((CH₃)₂CH). ³¹P{¹H} NMR (δ, CDCl₃, 20 °C): 142.7.

***N,N'*-Dihexyl-*N*-diphenylphosphino-2,6-diaminopyridine (2a').** *N,N'*-Dihexyl-2,6-diaminopyridine (1.6 g, 5.90 mmol) was dissolved

in diethyl ether and cooled to –70 °C. *n*-BuLi (5.90 mmol, 2.7 mL of a 2.20 M solution in hexane) was added slowly. The solution was allowed to reach room temperature and was then stirred for 1 h. After that, the solution was cooled to –10 °C, and ClPPh₂ (1.06 mL in 9 mL, 5.90 mmol) was added dropwise. The mixture was stirred overnight at room temperature. After that, the solution was filtered and the solvent was removed under vacuum. An orange oil was obtained. Yield: 2.3 g (87%). ¹H NMR (δ, CDCl₃, 20 °C): 7.45–7.35 (m, 11H, Ph and py⁴), 6.59 (dd, *J* = 8.0 Hz, *J* = 2.3 Hz, 1H, py³), 5.81 (d, *J* = 7.9, 1H, py⁵), 4.21 (bm, 1H, NH), 3.53–3.41 (m, 2H, CH₂NP), 3.21–3.13 (m, 2H, CH₂NH) 1.65–1.52 (m, 2H, CH₂), 1.44–1.19 (m, 8H, CH₂), 1.08–0.69 (m, 14H, CH₂ and CH₃). ³¹P{¹H} NMR (δ, CDCl₃, 20 °C): 47.8.

***N,N'*-Dihexyl-*N,N'*-bis(diphenylphosphino)-2,6-diaminopyridine (PNP-Ph^{Hexyl}) (2a).** This ligand has been prepared analogously to **2a'** with **2a'** (1.3 g, 2.86 mmol), PPh₂Cl (513 μL, 2.86 mmol), and *n*-BuLi (2.86 mmol, 1.24 mL of a 2.2 M solution in hexane) as the starting materials. Yield: 1.8 g (98%). ¹H NMR (δ, CDCl₃, 20 °C): 7.45–7.35 (m, 21H, Ph and py⁴), 6.77 (dd, *J* = 8.1 Hz, *J* = 2.4 Hz, 2H, py^{3,5}), 3.53–3.41 (m, 4H, CH₂N), 1.46–1.20 (m, 4H, CH₂) 1.05–0.70 (m, 18H, CH₂ and CH₃). ¹³C{¹H} NMR (δ, CDCl₃, 20 °C): 159.0 (py^{2,6}), 137.7 (py⁴), 132.6 (Ph), 128.7 (Ph), 128.3 (Ph) 100.0 (py^{3,5}), 48.0 (NCH₂), 31.3 (CH₂), 28.9 (CH₂), 26.7 (CH₂), 22.5 (CH₂), 13.9 (CH₃). ³¹P{¹H} NMR (δ, CDCl₃, 20 °C): 48.1.

***N,N'*-Diundec-10-enyl-*N*-bis(diphenylphosphino)-2,6-diaminopyridine (2b').** This ligand has been prepared analogously to **2a'** with undecaminopyridine (911 mg, 2.20 mmol), PPh₂Cl (396 μL, 2.20 mmol), and *n*-BuLi (2.20 mmol, 1 mL of a 2.2 M solution in hexane) as the starting materials. Yield: 1.3 g (98%). ¹H NMR (δ, CDCl₃, 20 °C): 7.47–7.21 (m, 11H, Ph and py⁴), 6.78 (dd, *J* = 8.1 Hz, *J* = 2.4 Hz, 2H, py^{3,5}), 6.60 (dd, *J* = 8.1 Hz, *J* = 2.4 Hz, 1H, py^{3,5}), 5.92–5.77 (m, 2H, CH=CH₂), 5.71 (d, *J* = 7.9 Hz, 2H, py^{3,5}), 5.05–4.93 (m, 4H, CH=CH₂), 4.23 (bm, 1H, NH), 3.51–3.42 (m, 2H, CH₂NP), 3.22–3.14 (m, 2H, CH₂N) 2.10–1.98 (m, 4H, CH₂), 1.63–1.55 (m, 2H, CH₂), 1.45–0.77 (m, 28H, CH₂ and CH₃). ³¹P{¹H} NMR (δ, CDCl₃, 20 °C): 47.9.

***N,N'*-Diundec-10-enyl-*N,N'*-bis(diphenylphosphino)-2,6-diaminopyridine (PNP-Ph^{Undec}) (2b).** This ligand has been prepared analogously to **2a** with **2b'** (887 mg, 1.48 mmol), PPh₂Cl (236 μL, 1.48 mmol), and *n*-BuLi (1.48 mmol, 674 μL of a 2.2 M solution in hexane) as the starting materials. Yield: 0.9 g (89%). ¹H NMR (δ, CDCl₃, 20 °C): 7.46–7.30 (m, 21H, Ph and py⁴), 6.75 (dd, *J* = 8.1 Hz, *J* = 2.5 Hz, 2H, py^{3,5}), 5.88–5.72 (m, 2H, CH=CH₂), 5.03–4.90 (m, 4H, CH=CH₂), 3.53–3.39 (m, 4H, CH₂), 2.05–1.96 (m, 4H, CH₂), 1.43–0.74 (m, 28H, CH₂). ¹³C{¹H} NMR (δ, CDCl₃, 20 °C): 159.1 (py^{2,6}), 139.2 (CH=CH₂), 138.0 (py⁴), 132.7 (Ph), 128.8 (Ph), 128.4 (Ph), 114.2 (CH₂=CH), 100.3 (py^{3,5}), 48.2 (NCH₂), 33.9 (=CHCH₂), 29.5(CH₂), 29.2(CH₂), 29.0(CH₂), 28.3-(CH₂), 28.1(CH₂), 28.0(CH₂), 27.1 (CH₂). ³¹P{¹H} NMR (δ, CDCl₃, 20 °C): 48.0.

***N,N'*-Bis(diphenylphosphino)-2,6-diamino-4-phenyl-1,3,5-triazine (PNP^T-Ph) (3).** A suspension of 2,6-diamino-4-phenyl-1,3,5-triazine (0.5 g, 2.67 mmol) in 30 mL of THF was treated with NEt₃ (0.82 mL, 5.88 mmol). After cooling to 0 °C a solution of PPh₂Cl (0.96 mL, 5.34 mmol) in 20 mL of THF was added dropwise. The suspension was warmed to room temperature and stirred overnight. After that, the precipitate was filtered off and the solvent removed under vacuum. The remaining white solid was used without further purification. Yield: 1.4 g (95%). ¹H NMR (δ, C₆D₆, 20 °C): 7.44–7.03 (m, 25H, Ph and PPh), 6.33 (s, 2H, NH). ¹³C{¹H} NMR (δ, C₆D₆, 20 °C): 171.9 (triaz⁴), 168.7 (dd, *J* = 17.0 Hz, *J* = 2.8 Hz, triaz^{2,6}), 139.6 (d, *J* = 15.6 Hz, PPh¹), 136.7 (Ph¹), 131.7 (d, *J* = 22.1 Hz, PPh^{2,6}), 131.7 (Ph⁴), 129.1 (PPh⁴), 128.5 (d, *J* = 6.9 Hz, PPh^{3,5}), 128.2 and 128.1 (Ph^{2,3,5,6}). ³¹P{¹H} NMR (δ, C₆D₆, 20 °C): 29.1.

[Mo(PNP-Prⁱ)(CO)₃](CH₃CN) (**4a**·CH₃CN). Mo(CO)₆ (300 mg, 0.88 mmol) in 10 mL of CH₃CN was refluxed in a Schlenk tube for 2 h. The yellow solution was cooled to room temperature and **1b** (233 mg, 0.88 mmol) was added. The mixture was stirred overnight at room temperature. Removal of the solvent afforded **4a** as a yellow solid. Yield: 420 mg (90%). Anal. Calcd for C₂₂H₃₆MoN₄O₃P₂: C, 46.98; H, 6.45; N, 9.96. Found: C, 46.89; H, 6.16; N, 9.12. ¹H NMR (δ, CD₃CN, 20 °C): 7.16 (t, *J* = 7.9 Hz, 1H, py⁴), 6.37 (bs, 2H, NH), 6.13 (d, *J* = 7.9 Hz, 2H, py^{3,5}), 2.45–2.18 (m, 4H, CH), 1.33–1.03 (m, 24H, CH₃). ¹³C{¹H} NMR (δ, CD₃CN, 20 °C): 231.4 (t, *J* = 5.8 Hz, CO), 216.9 (t, *J* = 10.4 Hz, CO), 161.0 (t, *J* = 7.8 Hz, py^{2,6}), 137.7 (py⁴), 97.1 (t, *J* = 3.1 Hz, py^{3,5}), 31.6 (t, *J* = 10.4 Hz, CH), 18.1 (t, *J* = 3.0 Hz, CH₃), 17.8 (t, *J* = 3.9 Hz, CH₃). ³¹P{¹H} NMR (δ, CD₃CN, 20 °C): 131.9. IR (KBr, cm⁻¹): ν_{C=O} 1938 (m, ν_{C=O}), 1907 (m, ν_{C=O}), 1824 (s, ν_{C=O}).

[Mo(PNP-Bu^t)(CO)₃](CH₃CN) (**4b**·CH₃CN). This complex has been prepared analogously to **4a** with [Mo(CO)₆] (512 mg, 1.97 mmol) and **1c** (782 mg, 1.97 mmol) as starting materials. The product was purified by chromatography (neutral Al₂O₃, eluent: CH₂Cl₂). Yield: 840 mg (74%). Anal. Calcd for C₂₆H₄₄MoN₄O₃P₂: C, 53.15; H, 7.55; N, 9.54. Found: C, 53.21; H, 7.17; N, 9.41. ¹H NMR (δ, CD₂Cl₂, 20 °C): 7.18 (t, *J* = 7.9 Hz, 1H, py⁴), 6.13 (d, *J* = 7.9 Hz, 2H, py^{3,5}), 5.25 (bs, 2H, NH), 1.42–1.35 (m, 36H, CH₃). ¹³C{¹H} NMR (δ, CD₂Cl₂, 20 °C): 223.1 (t, *J* = 9.6 Hz, CO), 207.3 (t, *J* = 8.4 Hz, CO), 160.6 (t, *J* = 6.5 Hz, py^{2,6}), 137.9 (py⁴), 97.8 (py^{3,5}), 39.9 (t, *J* = 5.0 Hz, CCH₃), 29.3 (d, *J* = 3.8 Hz, CH₃), 29.2 (d, *J* = 3.8 Hz, CH₃). ³¹P{¹H} NMR (δ, CD₂Cl₂, 20 °C): 148.8. IR (KBr, cm⁻¹): 1925 (s, ν_{C=O}), 1822 (s, ν_{C=O}), 1811 (s, ν_{C=O}).

[Mo(PNP-Prⁱ)(CO)₃](I₂) (**7a**). To a solution of **4a** (168 mg, 0.32 mmol) in 5 mL of CH₂Cl₂ was added 1 equiv of I₂ (82 mg, 0.32 mmol). Removing the solvent after 10 min afforded **7a** as a dark red solid. Yield: 230 mg (92%). Anal. Calcd for C₂₀H₃₃MoN₃O₃I₂P₂: C, 30.99; H, 4.29; N, 5.42. Found: C, 31.15; H, 4.16; N, 5.55. ¹H NMR (δ, CD₂Cl₂, 20 °C): 8.10 (bs, 2H, NH), 7.43–7.19 (m, 3H, py), 3.87–3.65 (m, 2H, CH), 3.14–2.84 (m, 2H, CH), 1.70–1.16 (m, 24H, CH₃). ³¹P{¹H} NMR (δ, CD₂Cl₂, 20 °C): 114.0. IR (KBr, cm⁻¹): 1969 (s, ν_{C=O}), 1938 (s, ν_{C=O}), 1858 (m, ν_{C=O}). If **4a** is treated with 2 equiv of I₂ under the same reaction conditions, [Mo(PNP-Prⁱ)(CO)₃](I₂)₂ (**7b**) was obtained, exhibiting NMR spectra identical with those of **7a**.

[Mo(PNP-Prⁱ)(CH₃CN)(CO)₂](I₂) (**8**). To a solution of **4b** (168 mg, 0.32 mmol) in 2 mL of CH₃CN was added 1 equiv of I₂ (82 mg, 0.32 mmol). The reaction mixture was stirred overnight at room temperature. **8** was isolated as a dark red microcrystalline precipitate. Yield: 120 mg (70%). Anal. Calcd for C₂₁H₃₆N₄O₂MoP₂: C, 47.20; H, 6.79; N, 10.48. Found: C, 47.44; H, 6.98; N, 10.76. ¹H NMR (δ, CD₃CN, 20 °C): 7.98 (bs, 1H, NH), 7.62–7.43 (m, 2H, NH, py⁴), 7.01 (d, *J* = 8.1 Hz, 1H, py³), 6.88 (d, *J* = 8.1 Hz, 1H, py³), 3.74–3.55 (m, 1H, CH), 3.05–2.84 (m, 3H, CH), not observed (3H, CH₃CN), 1.63–1.11 (m, 24H, CH₃). ³¹P{¹H} NMR (δ, CD₃CN, 20 °C): 113.8. IR (KBr, cm⁻¹): 2299 (w, ν_{C=N}), 2269 (w, ν_{C=N}), ν_{C=O} 1944 (s, ν_{C=O}), 1982 (s, ν_{C=O}), 1855 (m, ν_{C=O}).

[Fe(PNP-Ph)(CH₃CN)₃](BF₄)₂·3CH₃CN (**9a**·3CH₃CN). A solution of **1a** (500 mg, 1.05 mmol) and [Fe(H₂O)₆](BF₄)₂ (354 mg, 1.05 mmol) in acetonitrile (10 mL) was stirred at room temperature for 2 h. Insoluble materials were then removed by filtration, and the volume of the solution was reduced to about 2 mL. Upon addition of Et₂O, an orange precipitate was formed, which was washed twice with Et₂O and dried under vacuum. Yield: 805 mg (97%). Anal. Calcd for C₄₁H₄₆B₂F₈FeN₆O₂P₂: C, 51.50; H, 4.85; N, 13.18. Found: C, 51.24; H, 4.66; N, 13.35. ¹H NMR (δ, CD₃CN, 20 °C): 8.36 (s, 2H, NH), 7.91–7.62 (m, 21H, Ph, py⁴), 6.64 (d, *J* = 8.0 Hz, 2H, py^{3,5}), 1.97 (s, 9H, CH₃CN). ¹³C{¹H} NMR (δ, CD₃CN, 20 °C): 163.2 (t, *J* = 9.8 Hz, py^{2,6}), 141.2 (py⁴), 137.7

(CH₃CN), 136.7 (Ph), 131.5 (Ph), 131.0 (Ph), 129.2 (Ph), 100.9 (py^{3,5}), 3.4 (CH₃CN). ³¹P{¹H} NMR (δ, CD₃CN, 20 °C): 103.9.

[Fe(PNP-BIPOL)(CH₃CN)₃](BF₄)₂ (**9d**). This complex has been prepared analogously to **9a** with **1e** (2.0 g, 3.7 mmol) and [Fe(H₂O)₆](BF₄)₂ (1.3 g, 3.7 mmol) as the starting materials. Yield: 2.7 g (80%). Anal. Calcd for C₃₅H₃₀B₂F₈FeN₆O₂P₂: C, 47.23; H, 3.40; N, 9.44. Found: C, 47.10; H, 3.31; N, 9.55. ¹H NMR (δ, CD₃CN, 20 °C): 8.89 (s, 2H, NH), 7.84–7.81 (m, 14H, Ph), 7.24–7.21 (m, 1H, py⁴), 7.00–6.93 (m, 2H, Ph), 6.52 (d, *J* = 8.2 Hz, 2H, py^{3,5}), 2.32 (s, 6H, CH₃CN), 1.59 (s, 3H, CH₃CN). ¹³C{¹H} NMR (δ, CD₃CN, 20 °C): 159.9 (t, *J* = 13.2 Hz, py^{2,6}), 151.4 (Ph), 148.6 (Ph), 146.1 (py⁴), 142.7 (Ph), 137.7 (CH₃CN), 130.5 (Ph), 127.4 (Ph), 122.1 (Ph), 102.6 (py^{3,5}), 4.3 (CH₃CN). ³¹P{¹H} NMR (δ, CD₃CN, 20 °C): 186.7.

Deprotonation of [Fe(PNP-BIPOL)(CH₃CN)₃](BF₄)₂·CH₃CN (9d**·CH₃CN). Formation of [Fe(PNP-BIPOL)(CH₃CN)₃](BF₄)₂ (**12**). Method 1: A solution of **9d** (150 mg, 0.17 mmol) in acetonitrile was treated with an excess of NaHg (3%), whereupon an immediate formation of gas (H₂) took place. The mixture was stirred until the evolution of dihydrogen had ceased. Insoluble materials were then removed by filtration, and the solvent was evaporated under reduced pressure. The resulting dark brown solid was washed twice with Et₂O and dried under vacuum. Yield: 104 mg (76%). Method 2: A solution of **9d** (500 mg, 0.56 mmol) in acetonitrile was chromatographed over basic Al₂O₃, yielding a dark brown solution. Removal of the solvent under reduced pressure gave **12** as a dark brown solid. Yield: 367 mg (81%). Anal. Calcd for C₃₇H₃₂BF₄FeN₇O₄P₂: C, 52.70; H, 3.82; N, 11.63. Found: C, 52.55; H, 3.42; N, 11.98. The proton NMR spectrum was uninformative due to broad and featureless resonances. ¹³C{¹H} NMR (δ, CD₃CN, 20 °C): 158.9 (py^{2,6}), 149.0 (py⁴), 141.7 (CH₃CN), 130.3 (Ph), 129.8 (Ph), 127.0 (Ph), 122.2 (Ph), 101.7 (py^{3,5}), 4.1 (CH₃CN). Quaternary carbons could not be detected. ³¹P{¹H} NMR (δ, CD₃CN, 20 °C): 194.4.**

Reaction of 12 with HBF₄·OEt₂. Formation of [Fe(PNP-BIPOL)(CH₃CN)₃](BF₄)₂ (9d**). A 5 mm NMR tube was charged with **12** (30 mg, 0.04 mmol) in CD₃CN (0.5 mL). Upon addition of HBF₄·OEt₂ (2.3 μL, 0.04 mmol), the color of the solution changed from brown to orange. The reaction was monitored by ¹H and ³¹P{¹H} NMR spectroscopy, and quantitative formation of **9d** was observed.**

[Fe(PNP-Ph)(bipy)(CH₃CN)](BF₄)₂·CH₃NO₂ (**13**·CH₃NO₂). 2,2'-Bipyridine (28 mg, 0.18 mmol) was added to a solution of **9a** (150 mg, 0.18 mmol) in CH₃NO₂, whereupon the color of the solution immediately turned deep red. After the mixture was stirred at room temperature for 2 h, the solvent was evaporated in a vacuum, and the solid was precipitated, washed twice with Et₂O, and evaporated to dryness, yielding 154 mg (95%) of a deep red solid. Anal. Calcd for C₄₂H₃₉B₂F₈FeN₇O₂P₂: C, 52.26; H, 4.07; N, 10.16. Found: C, 52.76; H, 4.26; N, 9.98. ¹H NMR (δ, CD₃-NO₂, 20 °C): 8.66–8.64 (m, 2H, bipy¹), 8.57–8.54 (d, *J* = 8.2 Hz, 2H, NH), 8.11–8.06 (m, 2H, bipy⁴), 7.72–7.53 (m, 10H, Ph, py⁴), 7.43–7.37 (m, 2H, bipy^{2,3}), 7.18–6.75 (m, 11H, Ph), 6.49 (s, 2H, py^{3,5}), 1.68–1.67 (t, *J* = 1.48 Hz, CH₃CN). ¹³C{¹H} NMR (CD₃NO₂, δ): 163.2 (py^{2,6}), 156.8 (bipy⁵), 154.0 (bipy¹), 141.5 (py⁴), 138.0 (bipy³), 131.5 (Ph), 130.6 (Ph^{2,6}), 130.0 (Ph⁴), 129.3 (Ph^{3,5}), 128.7 (bipy⁴), 127.2 (CH₃CN), 123.6 (bipy²), 101.8 (py^{3,5}), 12.7 (CH₃CN). ³¹P{¹H} NMR (δ, CD₃NO₂, 20 °C): 101.8.

[Fe(PNP-Ph)(terpy)](BF₄)₂·CH₃NO₂ (**14**·CH₃NO₂). This complex was prepared analogously to **13** with 2,2':6',2''-terpyridine (42 mg, 0.18 mmol) and **9a** (150 mg, 0.18 mmol). Yield: 139 mg (83%). Anal. Calcd for C₄₅H₃₉B₂F₈FeN₆O₂P₂: C, 52.26; H, 3.98; N, 8.51. Found: C, 52.41; H, 4.10; N, 8.77. ¹H NMR (δ, CD₃-NO₂, 20 °C): 8:38 (m, 4H, terpy^{1,4}), 8.15 (s, 2H, NH), 7.75–7.72 (d, *J* = 7.8 Hz, 3H, terpy^{3,7}), 7.49–7.43 (t, *J* = 8.1 Hz, 2H, terpy⁶), 7.19–7.16 (m, 4H, terpy², py^{3,5}), 7.05–6.99 (m, 10H, Ph), 6.89–6.83 (m, 11H, Ph, py⁴). ¹³C{¹H} NMR (δ, CD₃NO₂, 20 °C): 163.3

(py^{2,6}), 157.6 (terpy⁸), 156.8 (terpy⁵), 152.8 (terpy¹), 141.6 (py⁴), 136.7 (terpy³), 136.3 (terpy⁷), 130.6 (Ph^{2,6}), 128.8–128.7 (Ph⁴, Ph), 127.0 (Ph^{3,5}), 123.2 (terpy⁴), 123.0 (terpy⁶), 122.0 (terpy²), 102.2 (py^{3,5}). ³¹P{¹H} NMR (δ, CD₃NO₂, 20 °C): 100.3.

[Fe(PNP-Ph)₂](BF₄)₂ (15). [Fe(H₂O)₆](BF₄)₂ (300 mg, 0.90 mmol) was added to a solution of **1a** (848 mg, 1.80 mmol) in THF, whereupon the color of the solution turned purple. After the mixture was stirred at room temperature for 2 h, the solvent was evaporated in a vacuum. The solid was precipitated, washed twice with Et₂O, and evaporated to dryness, yielding 960 mg (90%) of a purple solid. Anal. Calcd for C₅₈H₅₀B₂F₈FeN₆P₄: C, 58.82; H, 4.25; N, 7.10. Found: C, 59.04; H, 4.31; N, 6.98. ¹H NMR (δ, CD₃NO₂, 20 °C): 7.98–7.92 (t, *J* = 8.0 Hz, 2H, py⁴), 7.25–6.48 (m, 46H, Ph, py^{3,5}, NH). ¹³C{¹H} NMR (δ, CD₃NO₂, 20 °C): 163.0 (py^{2,6}), 142.1 (py⁴), 136.8 (Ph), 129.9 (Ph^{2,6}), 129.1 (Ph⁴), 128.8 (Ph^{3,5}), 101.6 (py^{3,5}). ³¹P{¹H} NMR (δ, CD₃NO₂, 20 °C): 92.0.

Ru(PNP-Ph)(PPh₃)Cl₂ (16a). A solution of **1a** (224 mg, 0.47 mmol) and [RuCl₂(PPh₃)₃] (450 mg, 0.47 mmol) in CH₂Cl₂ (6 mL) was stirred at room temperature for 2 h. The volume of the solution was reduced to about 1 mL. Upon addition of Et₂O, a light brown precipitate was formed, which was washed twice with Et₂O and dried under vacuum. Yield: 350 mg (82%). Anal. Calcd for C₄₇H₄₀Cl₂N₃P₃Ru: C, 61.92; H, 4.42; N, 4.61. Found: C, 62.09; H, 4.54; N, 4.70. ¹H NMR (δ, CD₂Cl₂, 20 °C): 7.50–6.35 (m, 31H, Ph, py²), 6.41 (d, *J* = 7.5 Hz, 2H, py^{1,3}), 5.95 (s, 2H, NH). ¹³C{¹H} NMR (δ, CD₂Cl₂, 20 °C): 159.2 (t, *J* = 7.4 Hz, py^{2,6}), 138.6 (py⁴), 137.7 (d, *J* = 39.5 Hz, PPh₃), 135.3 (t, *J*_{CP} = 23.0 Hz, PNP-Ph¹), 134.8 (d, *J* = 9.2 Hz, PPh_{2,6,3}), 133.4 (t, *J* = 5.5 Hz, PNP-Ph^{2,6}), 129.6 (PNP-Ph⁴), 128.6 (d, *J*_{CP} = 1.8 Hz, PPh_{4,3}), 127.2 (t, *J* = 4.6 Hz, PNP-Ph^{3,5}), 126.8 (d, *J* = 8.5 Hz, PPh_{3,5}), 98.5 (py^{3,5}). ³¹P{¹H} NMR (δ, CD₂Cl₂, 20 °C): 83.7 (d, *J* = 27.7 Hz, PNP), 38.2 (t, *J*_{PP} = 27.7 Hz, PPh₃).

[Ni(PNP-Ph)Br]Br (17a). To a solution of **1a** (463 mg, 0.97 mmol) in CH₂Cl₂ (10 mL) was added [NiBr₂(DME)] (300 mg, 0.97 mmol), and the mixture was stirred overnight at room temperature, whereupon an orange solid precipitated, which was collected on a glass frit, washed twice with Et₂O, and dried under vacuum. Yield: 620 mg (94%). Anal. Calcd for C₂₉H₂₅Br₂N₃NiP₂: C, 50.05; H, 3.62; N, 6.04. Found: C, 50.24; H, 4.16; N, 10.35. ¹H NMR (δ, CD₃OD, 20 °C): 7.89–7.48 (m, 21H, Ph, py⁴), 6.41 (d, *J* = 8.0 Hz, 2H, py^{3,5}), 3.30 (s, 2H, NH). ¹³C{¹H} NMR (δ, CD₃OD, 20 °C): 161.6 (py^{2,6}), 145.3 (Ph), 143.6 (py⁴), 132.5 (Ph^{2,6}), 132.3 (Ph⁴), 128.8 (Ph^{3,5}), 99.7 (py^{3,5}). ³¹P{¹H} NMR (δ, CD₃OD, 20 °C): 66.1.

[Ni(PNP-Prⁱ)Br]Br (17b). This complex has been prepared analogously to **17a** with NiBr₂(DME) (271 mg, 0.88 mmol) and **1b** (300 mg, 0.88 mmol) as the starting materials. Yield: 450 mg (81%). Anal. Calcd for C₁₇H₃₃Br₂N₃NiP₂: C, 36.47; H, 5.94; N, 7.50. Found: C, 36.24; H, 5.17; N, 7.25. ¹H NMR (δ, CD₃OD, 20 °C): 7.54 (t, *J* = 8.0 Hz, 1H, py⁴), 6.32 (d, *J* = 8.0 Hz, 2H, py^{3,5}), 3.30 (s, 2H, NH), 2.51–2.46 (m, 4H, CH(CH₃)₂), 1.53–1.36 (m, 24 H, CH(CH₃)₂). ¹³C{¹H} NMR (δ, CD₃OD, 20 °C): 161.8 (t, *J* = 8.9 Hz, py^{2,6}), 141.7 (py⁴), 97.4 (py^{3,5}), 24.9 (t, *J* = 13.7 Hz, CH(CH₃)₂), 14.2 (CH(CH₃)₂). ³¹P{¹H} NMR (δ, CD₃OD, 20 °C): 100.6.

[Ni(PNP-Bu^t)Br]Br (17c). This complex has been prepared analogously to **17a** with NiBr₂(DME) (233 mg, 0.75 mmol) and **1c** (300 mg, 0.75 mmol) as the starting materials. Yield: 440 mg (72%). Anal. Calcd for C₂₁H₄₁Br₂N₃NiP₂: C, 40.94; H, 6.71; N, 6.82. Found: C, 40.74; H, 6.89; N, 6.77. ¹H NMR (δ, CD₃OD, 20 °C): 7.51 (t, *J* = 8.1 Hz, 1H, py⁴), 6.36 (d, *J* = 7.9 Hz, 2H, py^{3,5}), 3.30 (s, 2H, NH), 1.59–1.52 (m, 36H, C(CH₃)₃). ¹³C{¹H} NMR (δ, CD₃OD, 20 °C): 163.4 (py^{2,6}), 143.0 (py⁴), 98.5 (py^{3,5}), 39.3 (t, *J* = 9.2 Hz, C(CH₃)₃), 27.3 (C(CH₃)₃). ³¹P{¹H} NMR (δ, CD₃OD, 20 °C): 103.7.

[Pd(PNP-Ph)Cl]Cl (18a). To a solution of [Pd(COD)Cl₂] (0.6 g, 2.1 mmol) in CH₂Cl₂ (10 mL) was added **1a** (1.0 g, 2.1 mmol).

After the mixture was stirred for 2 h, the solvent was removed under vacuum and the product was precipitated with Et₂O, collected on a glass frit, and washed twice with Et₂O (10 mL). Yield: 1.3 g (95%). Anal. Calcd for C₂₉H₂₅Cl₂N₃P₂Pd: C, 53.20; H, 3.85; N, 6.42. Found: C, 53.24; H, 3.57; N, 6.35. ¹H NMR (δ, CD₂Cl₂, 20 °C): 10.47 (s, 2H, NH), 8.00–7.28 (m, 21H, Ph, py⁴), 6.84 (d, *J* = 8.0 Hz, py^{3,5}). ¹³C{¹H} NMR (δ, CD₂Cl₂, 20 °C): 160.6 (t, *J* = 7.5 Hz, py^{2,6}), 151.1 (Ph), 142.0 (py⁴), 132.3 (t, *J* = 7.8 Hz, Ph^{2,6}), 130.1 (Ph⁴), 129.1 (t, *J* = 6.0 Hz, Ph^{3,5}), 101.7 (py^{3,5}). ³¹P{¹H} NMR (δ, CD₂Cl₂, 20 °C): 69.9.

[Pd(PNP-Prⁱ)Cl]Cl (18b). This complex has been prepared analogously to **18a** with [Pd(COD)Cl₂] (337 mg, 1.18 mmol) and **1b** (400 mg, 1.18 mmol) as the starting materials. Yield: 600 mg (98%). Anal. Calcd for C₁₇H₃₃Cl₂N₃P₂Pd: C, 39.36; H, 6.41; N, 8.10. Found: C, 38.98; H, 6.33; N, 8.25. ¹H NMR (δ, CD₂Cl₂, 20 °C): 9.44 (s, 2H, NH), 7.20 (t, *J* = 7.2 Hz, 1H, py⁴), 6.81 (d, *J* = 7.6 Hz, 2H, py^{3,5}), 2.67–2.56 (m, *J* = 6.8 Hz, 4H, CH(CH₃)₂), 1.44–1.32 (m, *J* = 8.7 Hz, 24 H, CH(CH₃)₂). ¹³C{¹H} NMR (δ, CD₂Cl₂, 20 °C): 162.4 (t, *J* = 6.1 Hz, py^{2,6}), 141.1 (py⁴), 100.4 (py^{3,5}), 27.3 (t, *J* = 13.4 Hz, CH(CH₃)₂), 17.3 (CH(CH₃)₂). ³¹P{¹H} NMR (δ, CD₂Cl₂, 20 °C): 108.4.

[Pd(PNP-Bu^t)Cl]Cl (18c). This complex has been prepared analogously to **18a** with [Pd(COD)Cl₂] (156 mg, 0.88 mmol) and **1c** (300 mg, 0.88 mmol) as the starting materials. Yield: 420 mg (81%). Anal. Calcd for C₂₁H₄₁Cl₂N₃P₂Pd: C, 43.88; H, 7.19; N, 7.31. Found: C, 43.91; H, 7.12; N, 7.35. ¹H NMR (δ, CD₂Cl₂, 20 °C): 9.43 (s, 2H, NH), 7.16 (d, *J* = 7.5 Hz, 2H, py^{3,5}), 6.95 (t, *J* = 7.2 Hz, 1H, py⁴), 1.55–1.49 (m, 36H, C(CH₃)₃). ¹³C{¹H} NMR (δ, CD₂Cl₂, 20 °C): 163.0 (t, *J* = 5.8 Hz, py^{2,6}), 140.6 (py⁴), 100.2 (py^{3,5}), 39.5 (t, *J* = 9.2 Hz, C(CH₃)₃), 28.0 (t, *J* = 3.2 Hz, C(CH₃)₃). ³¹P{¹H} NMR (δ, CD₂Cl₂): 115.7.

[Pd(PNP-ETOL)Cl]CF₃SO₃ (20a). KCF₃SO₃ (130 mg, 0.70 mmol) and [Pd(COD)Cl₂] (182 mg, 0.64 mmol) were added to a solution of **1d** (185 mg, 0.64 mmol) in CH₃CN. The mixture was stirred for 2 h and filtered. The yellow filtrate was evaporated to dryness, and the product was precipitated with Et₂O, collected on a glass frit, and washed twice with Et₂O (10 mL). Yield: 282 mg (76%). Anal. Calcd for C₁₀H₁₃ClF₃N₃O₇P₂PdS: C, 20.71; H, 2.26; N, 7.24. Found: C, 20.67; H, 2.36; N, 8.05. ¹H NMR (δ, CD₃CN, 20 °C): 7.54 (t, *J* = 8.4 Hz, 1H, py⁴), 6.20 (s, 2H, NH), 6.03 (d, *J* = 8.2 Hz, 2H, py^{3,5}), 4.36–4.30 (m, 8H, CH₂). ¹³C{¹H} NMR (δ, CD₃CN, 20 °C): 151.6 (py^{2,6}), 145.9 (py^{3,5}), 96.3 (py⁴), 67.7 (CH₂), 65.2 (CH₂). ³¹P{¹H} NMR (δ, CD₃CN, 20 °C): 123.8.

[Pt(PNP-Prⁱ)Br]Br (22a). To a solution of [Pt(COD)Br₂] (100 mg, 0.28 mmol) in CH₂Cl₂ (10 mL) was added **1b** (97 mg, 0.28 mmol). After the mixture was stirred for 2 h, the solvent was removed under vacuum and the product was precipitated with Et₂O, collected on a glass frit, and washed twice with Et₂O (10 mL). Yield: 184 mg (94%). Anal. Calcd for C₂₉H₂₅Br₂N₃P₂Pt: C, 41.85; H, 3.03; N, 5.05. Found: C, 41.49; H, 3.12; N, 5.21. ¹H NMR (δ, CD₂Cl₂, 20 °C): 9.43 (t, *J* = 15.2 Hz, 2H, NH), 7.16 (t, *J* = 8.1 Hz, 1H, py⁴), 6.95 (d, *J* = 8.0 Hz, 2H, py^{3,5}), 2.88–2.77 (m, 4H, CH(CH₃)₂), 1.41–1.34 (m, 24H, CH(CH₃)₂). ¹³C{¹H} NMR (δ, CD₂Cl₂, 20 °C): 161.7 (t, *J* = 5.5 Hz, py^{2,6}), 140.4 (py⁴), 100.0 (py^{3,5}), 27.3 (t, *J* = 17.0 Hz, CH(CH₃)₂), 17.2 (d, *J* = 9.2 Hz, CH(CH₃)₂). ³¹P{¹H} NMR (δ, CD₂Cl₂, 20 °C): 100.4 (t, *J*_{PP} = 1273 Hz).

[Pt(PNP-Bu^t)Br]Br (22b). This complex has been prepared analogously to **22a** with [Pt(COD)Br₂] (100 mg, 0.28 mmol) and **1c** (112 mg, 0.28 mmol) as the starting materials. Yield: 180 mg (85%). Anal. Calcd for C₂₁H₄₁Br₂N₃P₂Pt: C, 33.52; H, 5.49; N, 5.58. Found: C, 33.24; H, 5.42; N, 5.39. ¹H NMR (δ, CD₂Cl₂, 20 °C): 9.21 (t, *J* = 16.8 Hz, 2H, NH), 7.42 (t, *J* = 7.8 Hz, 1H, py⁴), 6.95 (m, 2H, py^{3,5}), 1.57–1.51 (m, 36H, C(CH₃)₃). ¹³C{¹H} NMR (δ, CD₂Cl₂, 20 °C): 162.0 (py^{2,6}), 140.2 (py⁴), 100.5 (py^{3,5}), 40.4 (t, *J* = 12.4 Hz, C(CH₃)₃), 28.6 (C(CH₃)₃). ³¹P{¹H} NMR (δ, CD₂Cl₂, 20 °C): 103.9 (t, *J*_{PP} = 1267 Hz).

X-ray Structure Determination. X-ray data for **4a**·CH₃CN, **4b**·CH₃CN, **7b**, **8**, **9a**·3CH₃CN, **9b**·solv, **9d**·solv, **9f**, **11**·3ClCH₂CH₂-Cl·H₂O, **12**·CH₃CN, **13**·solv, **14**·solv, **15**, **16d**·2CH₂Cl₂, **17a**·solv, **17c**·CH₃OH, **18c**·2CH₂Cl₂, and **20b**·(C₂H₅)₂O·2CH₃CN were collected on a Bruker Smart CCD area detector diffractometer using graphite-monochromated Mo K α radiation ($\lambda = 0.71073 \text{ \AA}$) and 0.3° ω -scan frames covering complete spheres of the reciprocal space. Corrections for absorption, $\lambda/2$ effects, and crystal decay were applied.²⁸ The structures were solved by direct methods using the program SHELXS97.²⁹ Structure refinement on F^2 was carried out with the program SHELXL97.¹⁸ All non-hydrogen atoms were refined anisotropically. Hydrogen atoms were inserted in idealized positions and were refined riding on the atoms to which they were bonded, using AFIX 137 orientation refinement for acetonitrile CH₃ groups. Badly disordered solvents were squeezed with the program PLATON prior to final refinement.³⁰ Further details including

(28) Bruker programs: *SMART*, version 5.054; *SAINT*, version 6.2.9; *SADABS*, version 2.10; *XPREP*, version 5.1; *SHELXTL*, version 5.1; Bruker AXS Inc.: Madison, WI, 2001.

(29) Sheldrick, G. M. *SHELX97*: Program System for Crystal Structure Determination; University of Göttingen: Göttingen, Germany, 1997.

(30) Spek, A. L. *PLATON*: A Multipurpose Crystallographic Tool; University of Utrecht: Utrecht, The Netherlands, 2004.

atomic parameters are given in the CIFs of the structures, which have been deposited as Supporting Information. Moreover, basic crystallographic data are given in Tables S1, S2, and S3 in the Supporting Information.

Acknowledgment. Financial support by the “Fonds zur Förderung der Wissenschaftlichen Forschung” is gratefully acknowledged (Project No. P16600-N11). D.B.-G. thanks the Basque Government (Eusko Jaurlaritz/Gobierno Vasco) for a doctoral fellowship.

Supporting Information Available: Synthesis and spectroscopic data of *N,N'*-di-10-undecenyl-2,6-diaminopyridine, *N,N'*-dihexyl-2,6-diaminopyridine, **4c**, **5**, **6**, **7c**, **9b**, **9c**, **9e**, **9f**, **10a**, **10b**, **11**, **16b–f**, **19a**, **19b**, **20b–e**, **21a**, **21b**, **23a**, and **23b**. Complete crystallographic data and technical details in tabular and in CIF format for **4a**·CH₃CN, **4b**·CH₃CN, **7b**, **8**, **9a**·3CH₃CN, **9b**·solv, **9d**·solv, **9f**, **11**·3ClCH₂CH₂Cl·H₂O, **12**·CH₃CN, **13**·solv, **14**·solv, **15**, **16d**·2CH₂Cl₂, **17a**·solv, **17c**·CH₃OH, **18c**·2CH₂Cl₂, and **20b**·(C₂H₅)₂O·2CH₃CN. This material is available free of charge via the Internet at <http://pubs.acs.org>.

OM0600644